



Cite this: *Lab Chip*, 2025, 25, 2129

Received 3rd October 2024,  
Accepted 2nd March 2025

DOI: 10.1039/d4lc00836g

[rsc.li/loc](https://rsc.li/loc)

## Light-based 3D printing and post-treatments of moulds for PDMS soft lithography†

Bastien Venzac 

Polydimethylsiloxane (PDMS) chips are still the workhorses of academic microfluidics. Their production requires the fabrication of moulds, commonly produced using clean-room technologies. Light-based 3D printing and in particular, vat photopolymerization, material jetting and two-photon polymerization are rising techniques for the fabrication of moulds for PDMS replication, thanks to their accessibility, fast prototyping time, and improving resolution. Here, we are first reviewing the possibility opened by 3D printing for soft lithography, with a focus on mould designs. Then, inhibition of PDMS curing by photosensitive resins will be discussed as the main technical hurdle of 3D printed moulds. Fortunately, mould post-treatments are efficient solutions to eliminate this curing inhibition, which we gathered in a large database of post-treatment protocols from the literature.

### Introduction: soft lithography

Polydimethylsiloxane (PDMS) is one of the preferred materials for microfluidic chip fabrication in academia. Among the ten most cited microfluidic articles, seven were based on PDMS chips according to Web of Science. PDMS has several properties that made it such a material of choice: transparency in the whole visible spectrum, low auto-fluorescence,<sup>1</sup> elastic and non-brittle behaviour,<sup>2</sup> and gas permeability.<sup>3,4</sup> After mixing a liquid base and a curing agent, PDMS cures and accommodates the shape of moulds in which it was poured, a technique called soft-lithography.<sup>5–7</sup> The transfer of micro and nanoscale features from a large variety of materials has been demonstrated, thanks to a low shrinkage during curing (1–2%).<sup>8</sup> Moulded PDMS is easily bonded to another PDMS, glass or silicon substrate using plasma bonding to create enclosed channels (see Fig. 1).<sup>9</sup> The PDMS flexibility also helps to create leak-free connections, by inserting large tubing inside a punched inlet.

However, PDMS also presents several disadvantages, including low chemical resistance and high swelling when in contact with a large variety of organic solvents,<sup>10</sup> strongly limiting its use for organic chemistry. Hydrophobic molecules easily adsorb to the PDMS surface, and small hydrophobic molecules can also be absorbed inside the material.<sup>11,12</sup> Surface treatments are often temporary, due to the migration of free silicone chains at the surface.<sup>13</sup> Finally,

soft lithography does not fit well for industrialization, as manufacturers prefer techniques allowing mass production like injection moulding or embossing.<sup>14</sup> Despite the development of a wide variety of new materials for microfluidic fabrication which answer some of these critics, PDMS might still be used abundantly in the future, due to the inertia for the adoption of new materials and the over-presence of PDMS in laboratories and the literature.<sup>15</sup>

One of the main reasons for its predominance in academia, specifically, is the possibility of creating microfluidic chips outside clean room environments with limited equipment. One silicon mould could be replicated in hundreds of chips using soft lithography, reducing the consumed time and price in clean rooms. PDMS replicas have also been used as intermediate moulds for further replication in harder materials (fused silica, thermoplastics, ...).<sup>16,17</sup> Soft lithography has been tested with various mould types, including etched silicon, SU8 patterns on silicon,<sup>18</sup> micro-milled brass or thermoplastics,<sup>19</sup> and even coins or leaves,<sup>20,21</sup> the latest being clean room-free.

In the search for cheaper and more accessible fabrication methods, moulds have been built using 3D printers. Fused deposition modelling, where a material is extruded from a nozzle, was tested as soon as 2002 with a thermoplastic material.<sup>22</sup> However, the low resolution of this technology impeded its adoption in the community, as surfaces contained 20–50 µm grooves and channels were hardly smaller than 500 µm with badly defined sections.<sup>23</sup> Since 2012, three 3D printing techniques based on photopolymerization of resins have been more and more frequently employed for mould fabrication: vat photo-polymerization (VP), material jetting (MJ) and two-photon polymerization

LAAS-CNRS, CNRS, Toulouse, France. E-mail: [bastien.venzac@laas.fr](mailto:bastien.venzac@laas.fr)

† Electronic supplementary information (ESI) available. See DOI: <https://doi.org/10.1039/d4lc00836g>



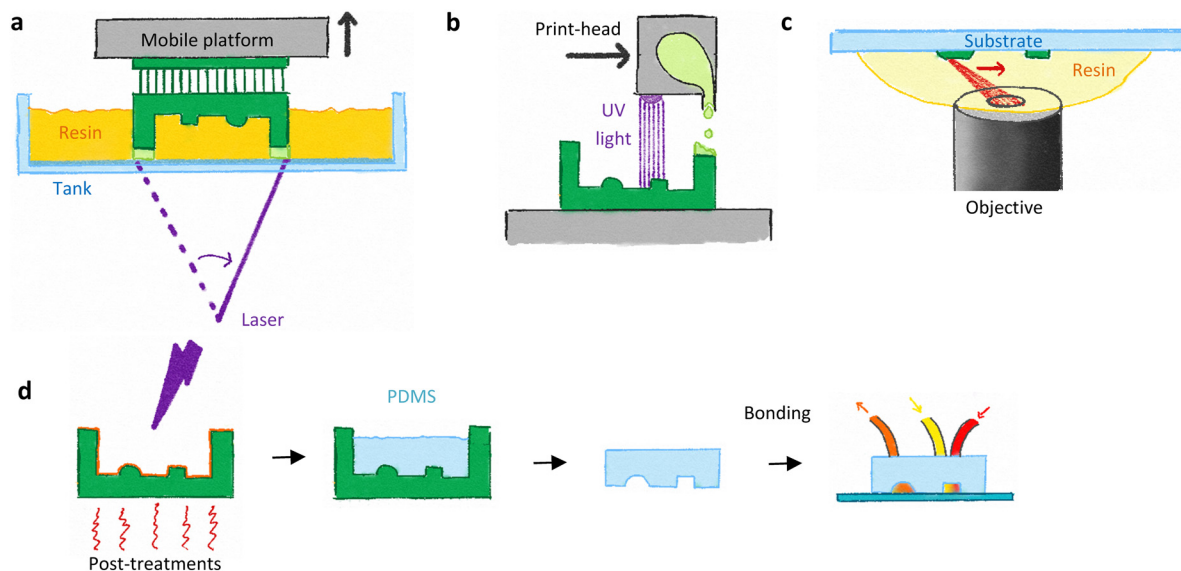


**Fig. 1** Schematic of the workflow of 3D printing for soft lithography. a) Stereolithography printing of a mould. b) Ink-jet printing of a mould. c) 2PP printing of a mould. d) Post-treatments, PDMS moulding and bonding of the PDMS replica on a glass slide for microfluidic chip fabrication.

(2PP). In this review, we will first describe in detail these 3 techniques. In a second section, examples of moulds will be provided and listed in increasing complexity, starting with 2D moulds, then 2.5D moulds producing a single plane of networks with different heights, and finishing with PDMS chips with multiple layers and fully 3D networks. Discussion about the perspectives of 3D printing for soft lithography will be presented. Finally, in a last section, a large database of post-treatment protocols for 3D printed moulds will be presented, to avoid both classical problems of PDMS curing inhibition and difficult removal of the PDMS replicas from the moulds.

## Section 1: light-based 3D printing techniques for soft lithography

### Vat polymerization

In vat polymerization, a thin layer (between 10 and 100  $\mu\text{m}$ ) of resin is photo-polymerized between a mobile build plate and a transparent tank. The light is patterned using a scanning laser in the case of stereolithography (SLA) or a projected image shaped by a micro-mirror array (Digital Light Processing, DLP) or by a liquid crystal display (LCD) screen masking the light from LEDs, with wavelengths between 350 and 550 nm (with a majority of printers at 405 nm). The photosensitive resins are mostly composed of acrylate or methacrylate monomers with additives, including photo-initiators and light absorbers. The platform then moves up by a layer thickness, and a new layer is polymerized below the previous one (see Fig. 1a). When overhangs are created, the thickness of the layer is given by the penetration length of the light, which depends on the dose and the concentration of light absorbers.

VP use for soft lithography has been rising since 2015; nowadays, VP printer prices are ranging from 200€ (Elegoo or Anycubic) to several tens of thousands of euros, with resolution going down to 30  $\mu\text{m}$  for standard commercial printers and below for academic prototypes or high resolution commercial machines.<sup>24–26</sup> For SLA, the print resolution and time are linked to the width of the laser beam, laser power and laser scan speed. Reducing the laser beam improves the resolution but increases strongly the printing time. Printing time is reduced using higher scanning speeds, but lead to lower doses which have to be compensated by a stronger laser. At the price of longer prints, both highly resolved and large moulds could be printed. In DLP printers, the resolution is directly linked to the pixel size of the projected image. Printing time is usually shorter than SLA, as a whole layer is cured in one exposure, and depends on the exposure time and light power. However, the print surface is dependent on the pixel number of the digital micro-mirror chips and manufacturers only provide chips with a resolution of up to 4 K (3840  $\times$  2160 pixels).<sup>27</sup> Therefore, a compromise between the print surface and resolution is mandatory. The last available technology, LCD printers, uses an LCD screen to mask light from LEDs. These low cost printers present the same advantages as the DLP printers, with the possibility of stitching several LCD screens to increase the print surface while keeping an identical resolution and low prices. However, these low-cost printers suffer from higher light inhomogeneity and lower power density, leading to lower performances and higher printing times.<sup>28</sup>

VP is an anisotropic fabrication process: the horizontal surfaces printed against the tank surface present a lower roughness than the vertical surfaces. In horizontal surfaces, small defects could be produced for SLA between laser passes if the hatching (the distance between two laser trajectories) is



too high. Defects appear in DLP or LCD at the pixel borders, since the light dose is often not fully constant from the pixel center to its borders. For VP in general, the tank surface are never totally flat, with a roughness of around 100 nm for a Formlabs 3B SLA printer and 200 nm for an Anycubic Photon DLP printer.<sup>29</sup> In vertical surfaces, grooves up to several tens of microns appear due to the vertical layers: in a single layer, the dose decreases along the light path thanks to light absorbers, leading to slight over-curing in the horizontal dimensions at the beginning of a layer.<sup>30</sup> Manufacturers often recommend tilting large horizontal surfaces to avoid suction on the tank when the build plate moves up, but this configuration produces a stair-like surface with steps having the same dimensions as the layers. Therefore, moulds are mostly printed horizontally, sometimes vertically,<sup>30</sup> with a limit on the total mould dimensions due to this suction effect that detaches the mould from the build plate. A usual solution to improve the adhesion to the build plate is to over-cure the first layers of the print. However, this over-curing also increases the shrinkage of the resin. If the mould is printed directly on the build plate, it results in a warped mould due to differential stress between the over-cured base and the rest of the mould.<sup>31</sup> This warping is reduced by increasing the mould thickness, or by adding support pillars and a base between the mould and the build plate to obtain a homogeneously cured mould.

After completion of the printing, the resulting object has to be removed from the build plate and washed to remove the unpolymerized resin, usually using isopropanol – some recent resins are washed with water.<sup>32,33</sup> Finally, most manufacturers recommend UV post-curing of the object, in order to fully complete the resin polymerization and improve the mechanical properties of the object.

### Material jetting

In MJ, an on-demand piezo-based print-head similar to an inkjet printer ejects drops of photosensitive resins on a horizontal surface. The print-head is able to move horizontally in 2 dimensions and deposit drops down to 16  $\mu\text{m}$  in diameter directly as lines of hundreds of droplets. After deposition, the resin is immediately cured by UV light located on the print-head. In this review, we will only describe inkjet printers working with photo-crosslinkable resins – other techniques used for 3D printing include the cooling of wax-based resins, the heating of thermoset drops or even the freezing of water-based resins.<sup>34,35</sup> Therefore, the resin has several requirements: low viscosity for the ejection of a drop with the appropriate diameter, a large increase of this viscosity on the cooled build plate to avoid the flowing of the printed layer, and photo-curing chemistry (often based on acrylate and urethane).<sup>36</sup> A subsequent layer of resin is then superimposed on the cured one until the print is finalized (see Fig. 1b). When overhanging structures have to be built, the use of a sacrificial support material is

required. Deposited from different nozzles in the same print-head, the support material is usually composed of water soluble resin, based on polyethylene glycol (Stratasys process) or on heat-removable wax (3D Systems process).<sup>35</sup>

MJ printing was the first mature commercial technology, leading to numerous reports for fabricating moulds before 2017.<sup>37–41</sup> All the examples found in the literature were based on commercial printers from Stratasys and 3D Systems, and their numbers decreased after 2017, as VP started to be more common and less expensive than MJ, where printers cost several tens of thousands of euros. In terms of performance, the lowest resolution obtained was around 100  $\mu\text{m}$ , with structures more rounded than VP, while the printing time was higher than VP (comparison between a Polyjet Eden 260VS and a Miicraft+ for the same design: 30 min vs. 12 min).<sup>23</sup>

### Two photon polymerization

For moulds containing small 3D features, below 50  $\mu\text{m}$ , a high-resolution 3D printing technique called two-photon polymerization (2PP) emerged in 2012.<sup>42</sup> In this technique, a drop of photosensitive resin is deposited on a horizontal surface, often a glass slide or a silicon wafer. A high numerical aperture objective focuses a light beam from a femtosecond laser inside the drop, either from the other side of the glass slide, or directly immersed in the resin drop. The resin does not cure at the wavelength of the laser but reacts with light having half this wavelength. Moreover, at the focal point of the laser, the photon density is particularly high, allowing simultaneous and non-linear absorption of two photons by the resin photo-initiators, leading to radical creation and photo-polymerization of the resin.<sup>43</sup> Since this two photon absorption is highly localized in the focal point, the polymerized voxel could be as small as  $200 \times 200 \times 600 \text{ nm}^3$ , and depends strongly on the objective used.<sup>44</sup> In the first commercial printers, the focal point is displaced in the liquid resin with a piezoelectric stage, allowing 3D, highly-precise but rather slow displacement with the unique possibility of following out-of-the-plane trajectories. In more recent generations, the focal point is displaced horizontally using galvanometric mirrors at high speed (up to  $100\,000 \mu\text{m s}^{-1}$ ) and the object is therefore built in a layer-by-layer fashion. At the end of the print, the unpolymerized resin is developed by immersing the glass slide in solvents, usually propylene glycol methyl ether acetate and then isopropanol. One practical hurdle of 2PP is to preserve the adhesion of the print on the glass slide, as the resins could shrink up to 10%.<sup>45</sup> This has been improved by silanizing the glass slide with methacrylated silanes, or by using other materials as supports (for example SU-8).<sup>46</sup>

While direct writing of solid epoxy resins has been demonstrated for the fabrication of microfluidic moulds since 2009,<sup>47</sup> the spread of commercial 2PP printers, particularly from the Nanoscribe company, has given rise to numerous reports of mould fabrication in the literature since



2017. Printers are now able to print with voxels varying between 200 nm and 2  $\mu\text{m}$  in width (Nanoscribe PPG2 and UpNano NanoOne 250). Identically to SLA, the same compromise has to be done between printing time and resolution. However, in contrast to SLA, the print size can be expanded in 2PP by stitching several fields of view, at the price of small defects at the stitching lines.<sup>44</sup> In general, 2PP is still considered as a slow technique, especially at its smaller voxel size, as moulds for typical microfluidic networks still need printing time above 10 hours. Hybrid techniques have been published, where only the zones requiring high resolution were built using 2PP.<sup>48,49</sup> The roughness of the prints depends mostly on the distance between two laser trajectories, and horizontal slices of 200 nm are observed.<sup>44</sup> Optimized writing trajectories allowed the creation of moulds with roughness compatible with optical components.<sup>50</sup>

### Replication in PDMS

After the mould is produced and developed, post-curing with UV-light is often used to improve the mechanical properties of the cured resin and to complete the conversion of the monomers, both in VP and 2PP.<sup>51</sup> The classical soft-lithography process includes mixing of the PDMS base and the curing agent, pouring of the mix on top of the moulds and removal of air bubbles with vacuum. For MJ and VP, the produced moulds sometimes include millimetre-high walls around the channels to contain the PDMS, allowing also the PDMS height to be controlled.<sup>52,53</sup> The PDMS is then usually cured at temperatures between 60 and 100 °C for several hours. Two main hurdles could then happen: for MJ and VP, most of the resins inhibit the PDMS curing, which is not the case for 2PP. Protocols have been developed to treat the moulds before pouring the PDMS, eliminating this curing inhibition. In section 3 of this review, we will discuss in detail the published post-treatments and propose an online and updated database of these protocols. These post-treatments are also sometimes required to facilitate the detachment of the PDMS replicas from the moulds. Among other tricks to improve the detachment, we advise to start detaching the PDMS from the resin mould with a scalpel, while adding isopropanol or ethanol below the replica. If the mould contains outer walls, an angle facilitates greatly the demoulding, as a lever can be produced with a scalpel on the side walls of the replica without damaging the horizontal surface. After removal of PDMS, the moulds could be re-used immediately.

## Section 2: examples of moulds

More and more laboratories are being equipped with 3D printers, and the temptation is high to 3D print moulds for soft lithography due to its numerous advantages compared to the main, classical clean room-based techniques. Infrastructure is not as heavy, except for 2PP which is still often located in clean rooms. The wide range of 3D printer

resolutions could create features at the limits of UV-based photo-lithography (2PP) and features of several hundreds of micrometres in all directions, which are now the typical dimensions of microfluidic or millifluidic applications like organ-on-chips.<sup>54</sup> Moulds comprising channels with different thicknesses or different geometries (rectangular, hemicylinders, half-spheres, ...) are easily created, in a prototyping time of less than half a day from design to use, and for prices which continue to quickly decrease while performances keep increasing.

In this section, we will give examples of the chip designs found in the literature using 3D-printed moulds, produced from VP, MJ or 2PP printers, starting with 2D moulds. Then, 2.5D moulds will be presented, showing already the great advantages of design freedom of 3D printing compared to lithography. More complex PDMS chips were produced using several moulds at once, allowing the fabrication of standing membranes and multilayer chips. The unique case of suspended channels with non-rectangular sections will then be discussed, finishing with the prospects of 3D printing for soft lithography.

### 2D moulds

A large proportion of the designs in the literature is still presenting channels with a single height, mimicking what is usual in classical photolithography, using SU-8 photoresists, dry films or other viscous, negative resists for thick patterns.<sup>55,56</sup> 3D printing use was mainly motivated by the simple access to this technology compared to clean-room techniques, its low prices or short prototyping times.<sup>57</sup> It can be compared, here, to maskless lithography methods in terms of advantages over classical photolithography.<sup>56,58</sup> Sometimes, chips with large channels, produced from macroscale moulds with features of several millimetres could simply not be done with clean-room techniques, limited to a few hundreds of micrometres.<sup>59</sup> The argument of a limiting resolution for 3D printing is less and less valid, as VP is more and more precise, as seen in Fig. 2a with the creation of pillars down to 50  $\mu\text{m}$   $\times$  50  $\mu\text{m}$   $\times$  200  $\mu\text{m}$  using a Sonic Mini 8K printer (Phrozen).<sup>52</sup> Moreover, with 2PP, 2D moulds have been produced with the same resolution as photolithography, but with more defined walls and wells.<sup>60</sup>

### 2.5D moulds

A classical improvement of SU-8 lithography is the fabrication of 2.5D moulds by stacking several thicknesses of resin on top to each other. Such moulds are rarely made of more than 3 layers, as the fabrication time increases linearly for each new layer. 3D printing allows the simple fabrication of moulds having as many different thicknesses as wished. Resulting PDMS channels with steps were used for the trapping of superabsorbent particles,<sup>64</sup> antibody-coated particles for diagnostics,<sup>65</sup> and zebrafish embryos.<sup>66</sup> For capillarity-based microfluidics, steps are efficient designs for trigger valves. Coupled with channels having different hydrodynamic





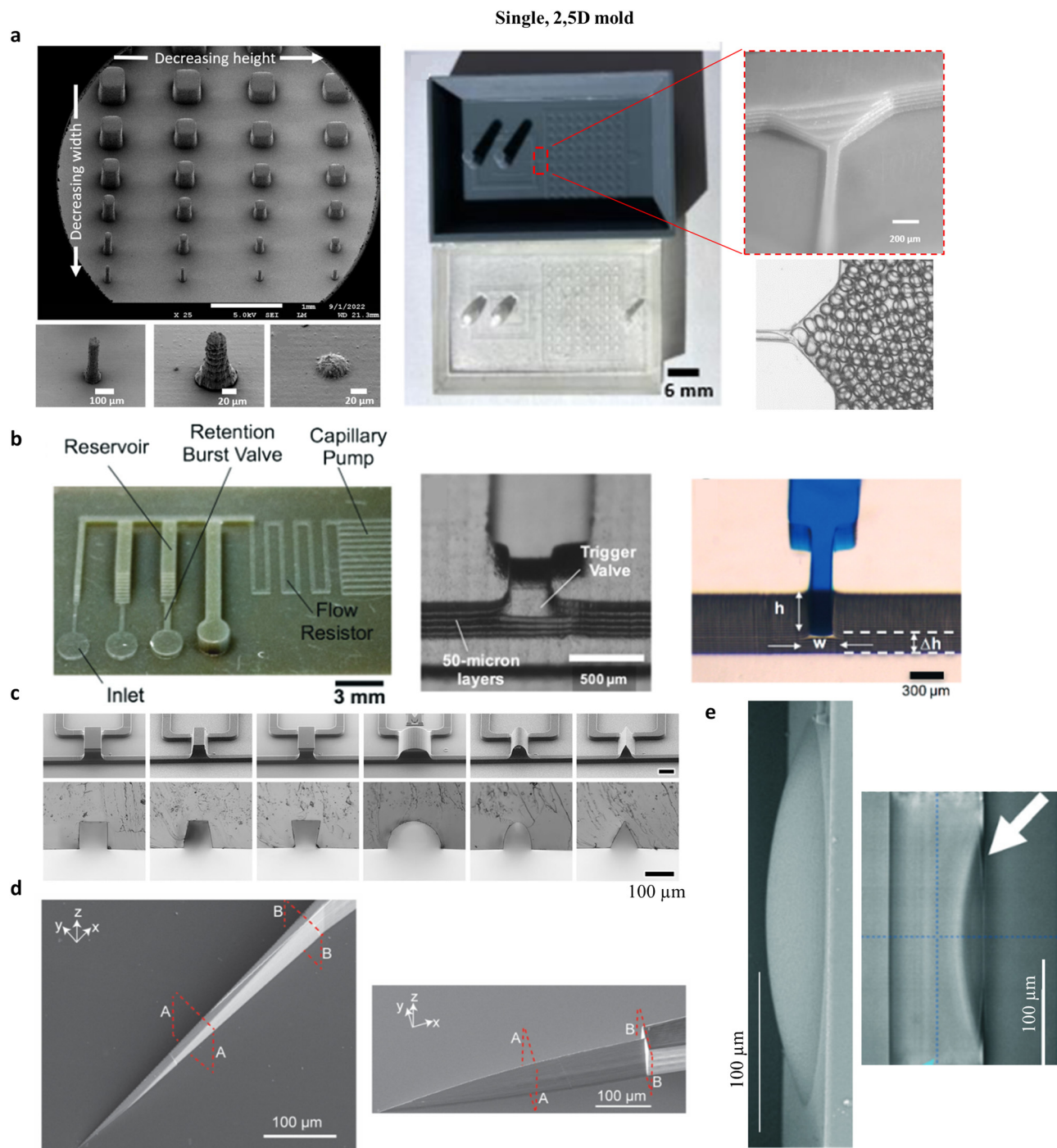


**Fig. 2** Examples of PDMS chips produced with a single, 2.5D mould. **a)** Left: Electronic micrograph of pillars produced with a Sonic Mini 8K (Phrozen) printer and Aqua Grey 8K (Phrozen) resin, showing pillars with setpoints of  $75 \times 75 \times 500 \mu\text{m}^3$ ,  $50 \times 50 \times 200 \mu\text{m}^3$ , and  $50 \times 50 \times 25 \mu\text{m}^3$ . Middle and right: Mould and PDMS replica following a thermal and silanization post-treatment. Right: Multilayer channel used for step emulsification. Adapted from [A. Vedhanayagam, 2023 (ref. 52)]. **b)** Left: 3D-printed mould showing multiple channel heights (printer Perfactory MicroEDU, resin Envisiontec HTM140). Middle and right: Images of the replicated PDMS chip, after treatment with a silicone coating, and demonstration of the multilayer channel as a trigger valve for capillary microfluidics. Adapted from [Olanrewaju, 2016 (ref. 61)]. **c)** Micrographs of 2PP moulds and cut PDMS replicas of channels with different geometries produced by 2PP (Nanoscribe PPGT, IP-S resin). Adapted from [Lamont, 2019 (ref. 62)]. **d)** Microblades produced by 2PP (Nanoscribe PPGT2, IP-S resin). Adapted from [Koppaka, 2021 (ref. 63)]. **e)** Micrographs, side view of moulds produced by 2PP (Nanoscribe PPGT, IP-S resin) (left) and top view of the resulting PDMS channel. Adapted from [Tang, 2020 (ref. 50)].

resistance thanks to different heights, these valves are part of pump-free and programmable microfluidic circuitry able to

flow several liquids sequentially for diagnostics (see Fig. 2c for pictures of the moulds and PDMS replicas).<sup>61</sup>



Moulds with slopes and curves were even more complicated to fabricate using usual clean-room techniques. Greyscale lithography has been developed, whether using grey-tone masks or direct laser writing with different laser powers in SU-8.<sup>67,68</sup> With 3D printers, moulds could present slopes and curves, as soon as the height of the structure is large compared to the slicing distance between two layers for VP printers, with the slices being less abrupt for MJ. As seen in Fig. 2a, a slope has been produced with a DLP printer to transfer droplets smoothly from a thin channel to a large reservoir. Here the slope is not fully smooth but presents more like a staircase profile due to the different layers.<sup>52</sup> We used a similar slope to help the transfer of *ex vivo* testis tissue from a well to a channel.<sup>54</sup> Slopes and curves have been used in several other applications, for example in hemi-cylindrical channels for valves (see Fig. 3a),<sup>69</sup> pyramidal or hemispherical wells for aggregation of cells into organoids,<sup>70,71</sup> or their fusions in well matrices,<sup>70,72</sup> or even in patterned surfaces for the guiding of neurons.<sup>71</sup>

Sometimes, really smooth slopes are required, and moving to 2PP printers is necessary as their slicing (when printing in a layer by layer fashion) is small enough to achieve gentle transitions.<sup>49,73,74</sup> Several channel profiles, 100  $\mu\text{m}$ -deep and wide, from rectangular, hemi-cylindrical

or triangular were produced by Lamont *et al.* and successfully replicated into PDMS using a Nanoscribe printer with a layer height of 1  $\mu\text{m}$  (Fig. 2c).<sup>62</sup> Micro-blades, with several sharp profiles, have been produced with 2PP. Slopes with angles of  $11^\circ$  and an aspect ratio of 10:1 were produced and replicated, as seen in Fig. 2d.<sup>63</sup> As a last example, 2PP also offers the possibility of finely tuning the shape of the PDMS channel wall themselves, for the fabrication of an optically smooth,  $200 \times 200 \mu\text{m}^2$  convex shape on the channel side for the creation of auto-aligned optical lenses (Fig. 2e).<sup>50</sup>

### Assembling multiple replicas or moulds

PDMS microfluidic chips are often made of several stacked replicas from several moulds, for example for creating pressure-based valves by S. Quake *et al.*<sup>75</sup> This simple idea was already presented in the first article showcasing the use of 3D printed moulds.<sup>37</sup> Liu *et al.* pushed it further away for the production of a pressure regulator, composed of 4 different PDMS replicas sandwiching two thin PDMS membranes, as seen in Fig. 3a.<sup>69</sup> Manufacturing the same chip using photolithography would have required a tedious process including four different wafers, one with two layers and one with three layers. With 3D printing, curved

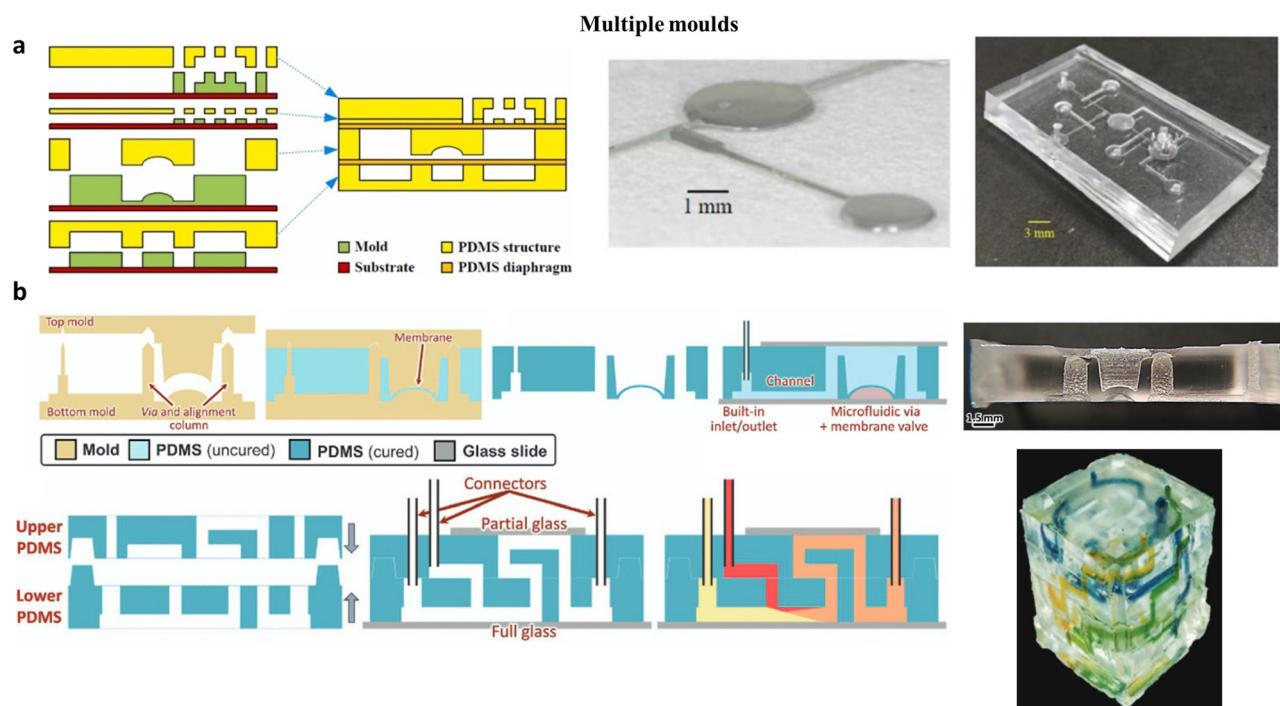


**Fig. 3** Examples of 3D PDMS chips produced using several moulds. a) Left: Schematic of the fabrication of the chip, using four different 3D printed moulds and stacking the resulting PDMS replicas with spin-coated membranes. Middle: Photographs of the 3D printed moulds, printed with a B9R-1-Cherry (B9Creations) resin and on a home-made DLP printer on a silanized glass slide, and then treated with extra UV and thermal curing. Right: Photograph of the final assembled chip. Adapted from [Liu, 2023 (ref. 69)]. b) Top left: Schematic of the one-step replication of a two-part mould with alignment structures printed with an MJ printer (ProJet 3000, 3DSystems and VisiJetEX200 resin) and treated with thermal baking and silanisation. Top right: Photograph of the resulting PDMS chip containing a membrane-based valve, cut in half. Bottom left: Schematic of the alignment of two 3D PDMS replicas produced with stacked moulds. Bottom right: Photograph of the resulting PDMS chips, made of 6 aligned layers. Adapted from [Glick, 2016 (ref. 41)].



channels for valves and elaborated outlets for chip-to-world connection were easily added. Assembling several PDMS replicas around porous and/or elastic membranes to produce multilayer chips is also usual in the organ-on-chip area, following the first example of a lung-on-chip by Huh *et al.*<sup>76</sup> This geometry has been produced from 3D-printed moulds, to mimic the lung,<sup>77</sup> oviduct,<sup>78</sup> or blood-brain-barrier culture conditions.<sup>79</sup>

When stacking replicas, aligning the layers during bonding is cumbersome, especially for complex circuitry like the one in Fig. 3a. Using an MJ printer, Glick *et al.* proposed in 2016 a one-step moulding of “multilayer-like” PDMS chips by stacking two 3D-printed moulds (see Fig. 3b, top), for the production of valves.<sup>41</sup> 3D alignment structures facilitated the assembly of the moulds. PDMS was poured inside the double mould, cured and then released. Floors and ceilings of the channels were made by bonding glass slides. This technique had multiple advantages: auto-alignment of the layers, production of thin membranes without spin coating, and reduction of labour with a single moulding process. The replicas also contained alignment structures, facilitating their stacking into a 6-layer chip, with each layer having 3D channels (see Fig. 3b, bottom).

### Suspended/3D moulds

In all the previous examples, the PDMS replicas were simply removed from 2.5D moulds by peeling them off. Cylindrical or even spiral channels have been produced by pulling out wires or fibres from cured PDMS, thanks to its elasticity.<sup>80,81</sup> Using 3D-printed templates, the same process produced channels with irregular sections and shapes, as shown in Fig. 4a.<sup>40</sup> Here, the mould was pulled out of the PDMS replica after removing the glass substrate below. This process also allowed the creation of channels with non-constant sections (Fig. 4b).<sup>53</sup> A blood vessel with an aneurism has been scanned and replicated in negative as a suspended structure. The suspended structure has been printed inside a container by SLA. After pouring and curing the PDMS, the links between the container and the suspended structure were broken, the PDMS was unmoulded and the structure was removed thanks to the PDMS elasticity. This PDMS channel, mimicking the original vessel, has then been used to test the aggregation of platelets in this patient-specific geometry. Sometimes, controlling the external shape of the PDMS replicas was also required. Two studies proposed to combine an internal mould and an external mould to

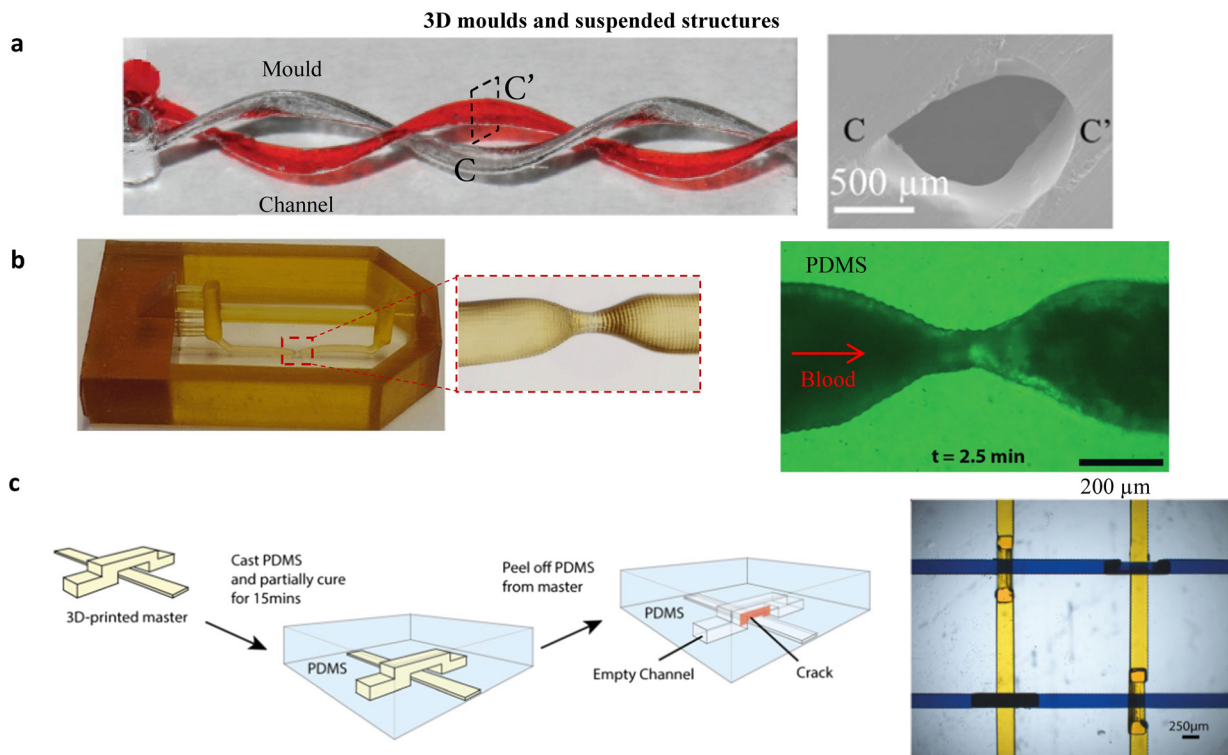


**Fig. 4** Examples of 3D PDMS chips produced from suspended structures. a) Left: Photograph of a PDMS replica containing one channel and one mould printed with an MJ printer (Objet24, Stratasys, and VeroWhitePlus resin) and coated with a gold–palladium layer. The mould was removed from the PDMS after curing. Right: Electronic micrograph of a channel cross section in PDMS. Adapted from [Hwang, 2015 (ref. 82)]. b) Left: Photographs of the mould printed using a SLA Perfactory 3 printer (EnvisionTec) and a PIC100 resin, treated with UV post-curing and washing in ethanol. Right: Blood perfusion inside a model of a stenotic vessel covered with endothelial cells to study the apparition of thrombosis. Adapted from [Costa, 2017 (ref. 53)]. c) Left: Schematic of the replication process. PDMS is partially cured on top of a 3D-printed mould containing suspended channels, printed using a Miicraft DLP printer and post-treated with thermal baking and silanisation. Before the complete curing of the PDMS, it is peeled off the master, forming a crack below the suspended channel which healed during the completion of the PDMS curing. Right: Example of crossing channels in the PDMS chip. Adapted from [Chan, 2015 (ref. 84)].



produce channels or tubes, with controlled wall thicknesses. In the first one, Hwang *et al.* produced soft robots, on which the wall thickness and geometry dictated the deflection of the robotic finger after pressurization of the internal channel.<sup>82</sup> Karam *et al.* needed to control finely the wall thicknesses of models of blood vessels to mimic the vessel deformability under pressure.<sup>83</sup>

An interesting proposition, mixing 2.5 and 3D moulding, has been shown by Chan *et al.* Their VP mould comprised not only extruded structures on a base, like a classical 2.5D mould, but also short suspended bridges above other channels, as seen in Fig. 4c. Here, PDMS was slightly under-cured, so the replica could be peeled off the mould, at the price of a crack under the overpassing channel, corresponding to the liberation of the suspended bridge. However, thanks to the curing properties of the PDMS, these cracks healed during the completion of the curing, creating in a single step complex circuitry with multilevel channels, without any leakage.<sup>84</sup>

### Perspectives and future of 3D printing for soft lithography

The use of 3D printers, and in particular VP, has skyrocketed in the last decade, pushed essentially by the increased availability of these printers in academic laboratories. Depending on the needs of each laboratory, the choice of the 3D-printing technology is crucial. Resolution in MJ is linked to the size of the ink drops, which depends on the nozzle geometry and viscosity of the ink. However, MJ printer optimization did not focus on resolution, but more on printing speed, print size and multi-material printing, with the last parameters being of small interest for mould manufacturing for soft lithography. Due to its large printing areas and printing speed, MJ printing is still a good choice when large-scale production of moulds with a resolution above 100  $\mu\text{m}$  is required, at the cost of a more expensive printer.

For VP, development has been more focusing on the resolution, where the smallest feature dimensions in X-Y depend mostly on the laser spot size for SLA or the pixel size for DLP. The resin composition, and in particular the presence of absorbers, has a larger influence on the z-resolution due to over-penetration of the light.<sup>35</sup> The smallest features below 10  $\mu\text{m}$  in X-Y have been demonstrated for projection micro stereolithography<sup>26,85</sup> and for laser-based SLA.<sup>24</sup> However, for one technology, decreasing the smallest feature dimensions always leads to a longer printing time. Recent advances in DLP demonstrated large area printed at sub-micron resolution, using stitching of the areas illuminated by a single micro-mirror array.<sup>26</sup> Further shortening the printing time of VP would mostly be possible by tuning the resin reactivity.<sup>28</sup>

Another important feature of VP is simply its reduced price, allowing laboratories to invest into a low-cost printer. In 2024, printer prices started at around 200\$ for Anycubic or Elego printers, with resolutions of 115  $\mu\text{m}$  and 50  $\mu\text{m}$  given

by the supplier specifications, at the cost of illumination heterogeneity, low irradiance and inconsistent prints, inconveniences which have been partly reduced using optimized inks.<sup>28,86</sup>

To significantly decrease the resolution or printing time of moulds, one should check the development of other light-based 3D-printing technologies. Whereas commercial 2PP is still a slow printing technique compared to VP at its maximum resolution, numerous academic developments around this technology are significantly increasing its throughput, using multi-focus,<sup>87</sup> two step-absorption,<sup>88,89</sup> holographic 2PP,<sup>90</sup> as reviewed by Balena *et al.*<sup>91</sup> In another direction, several occurrences of volumetric 3D printing have been published since 2019, where volumes (and not layers) of resin are directly photo-polymerized through tomographic projections,<sup>92</sup> or the intersection of two light beams of different colours, in combination with a dual colour photo-initiator.<sup>93</sup> These strategies promised printing speed several orders of magnitude higher than VP, with resolution on the same scale.

In conclusion of this section, light-based 3D printing has already proven useful for the fabrication of mould for soft lithography. With the next generations of technologies, including more precise VP, high-speed 2PP or volumetric printing, 3D printing might overcome clean-room based mould fabrication techniques, as the smallest printable features and printing time will continue to decrease.

## Section 3: PDMS curing inhibition by 3D printed moulds: protocol database

Is everything so easy with 3D printing? Not necessarily. In fact, one of the main drawbacks of VP and MJ is that PDMS does not cure correctly when in contact with most of their resins, leading to a layer of uncured PDMS around the channels that makes the mould useless. The main commercial silicone, Dow Corning Sylgard 184, is a complex mixture which contains a mix of linear polydimethylsiloxane with vinyl ends, branched siloxanes and platinum-based catalysts.<sup>94</sup> On the other hand, commercial VP and MJ resins are industrial secrets, but most resins are based on radical systems, mostly (meth)acrylates or thiol-ene, sometimes mixed with cationic systems, like epoxides, oxetanes or vinyl ethers.<sup>35</sup> We checked the composition of 12 resins from 12 different suppliers through their SDS documents: Anycubic Standard resin+,<sup>95</sup> 3D systems Eggshell AMB 10,<sup>96</sup> B9Creations B9R-1-Cherry,<sup>97</sup> DWS DL260,<sup>98</sup> Elegoo ABS-like,<sup>99</sup> Envisiontec PIC100,<sup>100</sup> Formlabs Clear v4,<sup>101</sup> Fun-To-Do Industrial Blend,<sup>102</sup> LiqCreate Premium Tough,<sup>103</sup> Phrozen Aqua Grey 8K,<sup>104</sup> Resione HT100,<sup>105</sup> and Stratasys VeroWhite + RGD835.<sup>106</sup> All of them reported the presence of acrylate or methacrylate monomers, with additional epoxy monomers for 3 of them. 9 SDS out of 12 indicated the presence of phosphine oxide-based photo-initiators. Care has to be taken as only “dangerous” chemicals are listed there.





**Table 1** Post-treatments including only UV post-curing

		UV post-curing			
Reference	Resin	Duration	Wavelength	Dose	Temperature
VAT photopolymerization					
Razavi Bazaz <sup>57</sup>	Creative CADWorks, custom resin	X	405 nm	X	X
Venzac <sup>111</sup>	DWS, GL4000	4 h	405 nm	14 mW cm <sup>-2</sup>	60 °C
Venzac <sup>111</sup>	Formlabs, Flex v1	2 h	405 nm	14 mW cm <sup>-2</sup>	60 °C
Hagemann <sup>71</sup>	Phrozen, Aqua Grey 4K	1 h	405 nm	X	X
Vogt <sup>114</sup>	Formlabs, Black RS-F2-GPBK-04	24 h	X	X	X
Cameron <sup>79</sup>	Creative CADWorks, Master Mold Resin	60–80 min	405 nm	5.5 mW cm <sup>-2</sup>	RT
Cameron <sup>79</sup>	Formlabs, Clear RS-F2-GPCL-04	1 h	405 nm	5.5 mW cm <sup>-2</sup>	60 °C
Lundquist <sup>113</sup>	Formlabs, BioMed Clear	1 h	405 nm	5.5 mW cm <sup>-2</sup>	60 °C
Som Yang <sup>115</sup>	Formlabs, Clear FLGPCL04	15 min	405 nm	5.5 mW cm <sup>-2</sup>	RT
Som Yang <sup>115</sup>	Formlabs, Surgical Guide FLSGAM01	15 min	405 nm	5.5 mW cm <sup>-2</sup>	RT
Material jetting					
Cutuli <sup>116</sup>	Stratasys, Vero PureWhite RDG837	1 h	X	X	37 °C

X corresponds to data unavailable in the references.

In the literature, several molecules have been shown to poison the platinum catalysts used in PDMS, including maleate, fumarate,<sup>107</sup>  $\beta$ -alkynol,<sup>108</sup> tri-organophosphite,<sup>109</sup> or sulfur-containing molecules like benzothiazole.<sup>110</sup> In particular, we have shown in a previous study that mixing phosphine oxide-based photo-initiators (TPO and BAPO) with PDMS resulted in complete inhibition of the silicone curing.<sup>111</sup> This analysis was supported by other experiments, showing that the leaching of fragments of phosphine oxide-based photo-initiators from the moulds to the PDMS is likely the cause of the PDMS curing inhibition from 3D-printed moulds. The absence of this class of photo-initiators in 2PP resins is probably the main reason for the absence of curing inhibition from these resins.<sup>35</sup> We did not show any

significant inhibition from monomers (methyl-methacrylate) but rather a stronger bond between a cured, acrylate-contaminated PDMS part and 3D-printed mould. Therefore, two effects of leachates from moulds have to be reduced with post-treatments: first, the PDMS curing inhibition and second, potential bonding between the PDMS and the printed mould.

This increase of bonding between 3D printed moulds and PDMS has been shown, independently of the PDMS inhibition, for a large spectrum of resin formulation. Coupled with the presence of a larger roughness on the vertical surfaces, demoulding PDMS can be tricky, and the literature contains many protocols to decrease this adhesion, using mostly fluorinated silanes, and release chemicals. This is also the case with 2PP moulds, where a slight increase of adhesion can break these fragile moulds due to the weak adhesion of the printed structures on the substrate (often a glass slide or silicon substrate).

In the next sections of this article, we propose to review all the protocols for treating 3D printed moulds and to class them into different classes of protocols. Since the first reported use of SLA-printed moulds in 2013 (ref. 37) and MJ-printed moulds in 2014,<sup>38,39</sup> multiple protocols have been proposed to alleviate the PDMS curing inhibition observed with the vast majority of photosensitive resins. Most publications did not study in detail this phenomenon and proposed a simple protocol, without discussing its optimization. Some other studies, including ours, focused on that specific question.<sup>71,111,112</sup> In total, at the submission of this review, we found in the literature 136 different post-treatments with enough details to be replicated, for 75 different resins. Here, we propose a review of the main routes used to treat 3D printed moulds and their mechanisms and offer a database containing all these protocols. Along this publication, we propose to maintain and expand further this list in the future as an open access database available at the following DOI: <https://doi.org/10.5281/zenodo.13881893>. New published protocols could be directly sent to the

**Table 2** Post-treatments including only thermal baking

Reference	Resin	Thermal baking	
		Duration	Temperature
VAT photopolymerization			
Venzac <sup>111</sup>	DWS, DL260	1 h at 120 °C or 24 h at 60 °C	
Venzac <sup>111</sup>	DWS, DS3000	2 h at 120 °C or 24 h at 60 °C	
Venzac <sup>111</sup>	Envisiontec, E-shell 300	1 h at 120 °C or 24 h at 60 °C	
Venzac <sup>111</sup>	Formlabs, Black v1	1 h at 120 °C or 24 h at 60 °C	
Venzac <sup>111</sup>	Formlabs, Clear v1	1 h at 120 °C or 24 h at 60 °C	
Venzac <sup>111</sup>	Formlabs, Flex v1	2 h	120 °C
Venzac <sup>111</sup>	Formlabs, High Temperature v1	1 h at 120 °C or 1 h at 60 °C	
Kang <sup>117</sup>	Formlabs, Clear	1 h	120 °C
Sanchez <sup>118</sup>	Formlabs, Black	Overnight	60 °C
Material jetting			
Stolovicki <sup>119</sup>	Objet, unspecified	Overnight	90 °C
Cicolini <sup>120</sup>	Stratasys, VeroWhite	Overnight	110 °C
Segantini <sup>121</sup>	Stratasys, VeroWhite	12 h	110 °C
Mossoti <sup>122</sup>	Stratasys, VeroWhite	Overnight	110 °C
2-Photon polymerization			
Tang <sup>50</sup>	Nanoscribe, IP-S	2 h	200 °C



**Table 3** Post-treatments including UV post-curing and thermal baking

Reference	Resin	UV post-curing				Thermal baking	
		Duration	Wavelength	Dose	Temperature	Duration	Temperature
VAT photopolymerization							
Dinh <sup>123</sup>	Da Vinci Nobel 1.0A resin	X	X	X	X	24 h	80 °C
Grigorov <sup>112</sup>	Anycubic, basic	4 min	395 nm	X	X	1 h	80 °C
Grigorov <sup>112</sup>	Anycubic, plant based	4 min	395 nm	X	X	1 h	80 °C
Grigorov <sup>112</sup>	Elegoo, ABS-like	4 min	395 nm	X	X	2 h	80 °C
Grigorov <sup>112</sup>	Phrozen, Aqua 4K	4 min	395 nm	X	X	2 h	80 °C
Jóskowiak <sup>124</sup>	Formlabs, Grey	1 h	405 nm	5.5 mW cm <sup>-2</sup>	60 °C	72 h	65 °C
Karam <sup>83</sup>	3D Systems, Eggshell-Amb10	90 min	X	X	X	1 h, 60 °C before UV/30 min, 80 °C after UV	
Lee <sup>125</sup>	Formlabs, Clear v4	1 h	X	X	X	2 h	120 °C
Liu <sup>69</sup>	B9Creations, B9R-1-Cherry	1 h	X	X	X	1 h	100 °C
Može	Fun-to-do, Industrial Blend Unpigmented	6 min	365–405 nm	900 mW cm <sup>-2</sup>	X	4 h	100 °C
Može	Fun-to-do, Deep Black	6 min	365–405 nm	900 mW cm <sup>-2</sup>	X	4 h	100 °C
Može	Phrozen, Aqua Grey 8K	10 min	365–405 nm	900 mW cm <sup>-2</sup>	X	4 h	100 °C
Memarian <sup>126</sup>	Phrozen, Aqua Gray 8K	45 min	X	X	RT	4 h	100 °C
Le Gac <sup>127</sup>	Formlabs, Clear v4	1 h	405 nm	5.5 mW cm <sup>-2</sup>	60 °C	2 h	120 °C
Le Gac <sup>127</sup>	Formlabs, High Temp v2	2 h	405 nm	5.5 mW cm <sup>-2</sup>	60 °C	4 h	120 °C
Le Gac <sup>127</sup>	Formlabs, BioMed	30 min	405 nm	5.5 mW cm <sup>-2</sup>	60 °C	2 h	120 °C
Le Gac <sup>127</sup>	Formlabs, surgical grade	1 h	405 nm	5.5 mW cm <sup>-2</sup>	60 °C	2 h	120 °C
Le Gac <sup>127</sup>	Formlabs, Elastic 50A	6 h	405 nm	5.5 mW cm <sup>-2</sup>	60 °C	48 h	120 °C
Le Gac <sup>127</sup>	Anycubic, plant-based	1 h	405 nm	5.5 mW cm <sup>-2</sup>	60 °C	2 h	120 °C
Le Gac <sup>127</sup>	Elegoo, plant-based	1 h	405 nm	5.5 mW cm <sup>-2</sup>	60 °C	2 h	120 °C
Le Gac <sup>127</sup>	eSUN, eResin	1 h	405 nm	5.5 mW cm <sup>-2</sup>	60 °C	2 h	120 °C
Le Gac <sup>127</sup>	BASF, Ultracur3D RG 35	1 h	405 nm	5.5 mW cm <sup>-2</sup>	60 °C	2 h	120 °C
Le Gac <sup>127</sup>	BASF, Ultracur3D ST 45 M	1 h	405 nm	5.5 mW cm <sup>-2</sup>	60 °C	2 h	120 °C
Ramasamy <sup>29</sup>	Anycubic, Black (SKU TL4425)	30 min	405 nm	5.5 mW cm <sup>-2</sup>	60 °C	2 h	120 °C
Ramasamy <sup>29</sup>	Formlabs, Clear v4 (RS-F2-GPCL-04)	30 min	405 nm	5.5 mW cm <sup>-2</sup>	60 °C	2 h	120 °C
Venzac <sup>111</sup>	DWS, GL4000	1 h	405 nm	14 mW cm <sup>-2</sup>	60 °C	8 h	120 °C
Venzac <sup>111</sup>	DWS, GM08	1 h	405 nm	14 mW cm <sup>-2</sup>	60 °C	8 h at 120 °C or 24 h at 60 °C	
Venzac <sup>111</sup>	Envisiontec, PIC100	2 h	405 nm	14 mW cm <sup>-2</sup>	60 °C	4 h	120 °C
Venzac <sup>111</sup>	Envisiontec, R11	2 h	405 nm	14 mW cm <sup>-2</sup>	60 °C	4 h	120 °C
Venzac <sup>111</sup>	Fun-to-do, Deep Black	15 min	405 nm	14 mW cm <sup>-2</sup>	60 °C	2 h at 120 °C or 48 h at 60 °C	
Venzac <sup>111</sup>	Fun-to-do, Industrial Black	15 min	405 nm	14 mW cm <sup>-2</sup>	60 °C	2 h	120 °C
Venzac <sup>111</sup>	Fun-to-do, Industrial Red	15 min	405 nm	14 mW cm <sup>-2</sup>	60 °C	2 h at 120 °C or 48 h at 60 °C	
Venzac <sup>111</sup>	Fun-to-do, Standard Black	1 h	405 nm	14 mW cm <sup>-2</sup>	60 °C	4 h	120 °C
Venzac <sup>111</sup>	Fun-to-do, Standard red	2 h	405 nm	14 mW cm <sup>-2</sup>	60 °C	8 h	120 °C
Yang <sup>128</sup>	Cyanate custom resin with a perfluoropolyether release agent	20 min	X	3 mW cm <sup>-2</sup>	X	1 h at 100 °C then 2 h at 140 °C then 2 h at 160 °C then 2 h at 180 °C then 2 h at 200 °C	



Table 3 (continued)

Reference	Resin	UV post-curing				Thermal baking	
		Duration	Wavelength	Dose	Temperature	Duration	Temperature
Som Yang <sup>115</sup>	Formlabs, Elastic 50A (FLELCL01)	15–45 min	405 nm	5.5 mW cm <sup>-2</sup>	RT	8 h	80 °C
Som Yang <sup>115</sup>	Formlabs, Elastic 80A (FLFL8001)	15–45 min	405 nm	5.5 mW cm <sup>-2</sup>	RT	8 h	80 °C
Ye <sup>66</sup>	Anycubic, Gray UV	2 h	X	X	X	16 h	80 °C
Hu <sup>129</sup>	Formlabs, Clear	30 min	X	X	X	2 h	120 °C
Lee <sup>130</sup>	3D Systems, Nextdent Ortho Rigid	1 h	X	X	X	2 h	100 °C
Khoo <sup>131</sup>	Formlabs, Clear v4 resin (RS-F2-GPCL-04)	30 min	405 nm	5.5 mW cm <sup>-2</sup>	60 °C	1 h	120 °C
Chen <sup>132</sup>	Formlabs, Durable	30 min	405 nm	5.5 mW cm <sup>-2</sup>	RT	24 h	65 °C
Byrne <sup>133</sup>	Formlabs, Clear resin	15 min	405 nm	5.5 mW cm <sup>-2</sup>	RT	3 h	130 °C

X corresponds to data unavailable in the references.

corresponding author at bastien.venzac@laas.fr to be added into the database.

### UV-post curing

VP manufacturers advise short post-curing of the print under UV light, at the same wavelength as the printer light, often at 405 nm. In order to obtain the best resolution, the light dose applied during printing is just above the polymerization threshold of the resin, meaning that only a fraction of the active sites of the monomers reacted. To improve the mechanical properties of the printed object and complete the resin polymerization, a UV post-curing step is often required, especially for (meth)acrylate systems.<sup>35,51</sup> We have previously shown, using Raman spectroscopy of moulds, that UV post-curing reduced methacrylate and acrylate groups in the mould.<sup>111</sup> One drawback of UV post-curing is the short penetration length of the light inside the printed objects, due to the necessary presence of photo-absorbers in the resin. UV post-curing might not reach the core of thick prints. Eleven post-treatments consisting only of UV-post curing have been found (see Table 1), almost all for VP, with treatment duration longer than the manufacturer recommendation for routine post-curing, from 15 min to 24 h.<sup>57,71,79,111,113–116</sup> Unfortunately, the method sections of most articles are incomplete, with missing information on UV wavelengths, treatment duration and/or dose applied. Several articles used a commercial curing box, optimized for multi-angle illumination of prints and available at reasonable costs, making such a post-treatment step quite standard for labs equipped with VP 3D printers. Beware, UV wavelength is an important parameter, as 254 nm or 365 nm UV light does not often cure resins that polymerize at 405 nm.

### Thermal baking only

Another classical post-treatment is a thermal baking step after the development of the moulds, at temperatures ranging from 60 to 200 °C. For cationic systems, heat has the

same effect as UV post-curing and completes the polymerization of the monomers, with the advantage of treating also the printed part beyond the UV penetration length.<sup>35</sup> In a previous study, we have shown that thermal baking of moulds for 4 different resins is accompanied by a decrease of mass around 1% and by the evaporation of a liquid containing mainly fragments of the photo-initiator, and sometimes (meth)acrylate monomers. When mixed with PDMS, this liquid inhibits the PDMS curing. We have also shown that thermal baking promotes the rearrangement of photo-initiator fragments into larger molecules.<sup>111</sup> Therefore, thermal baking could limit the PDMS curing inhibition through two phenomena: evaporation of small fragments of phosphine oxide-based photo-initiators outside of the moulds and trapping of the remaining fragments inside the moulds to limit their leaching. Fourteen different post-treatments have been sorted, for eleven different resins, as seen in Table 2. Compared to UV-curing, only an oven or a hotplate is necessary for this simple treatment. The choice of temperature and duration has to be tested by trial and error, starting with a high temperature of around 100–120 °C and at least 4 hours, and then reducing the duration or temperature if the treatment is efficient. However, high baking temperature could significantly warp or even crack moulds for some resins, especially without UV post-curing. Fortunately, lower baking temperatures are usually also efficient, at the price of longer treatment durations. Indeed, we have observed that an imperfectly treated mould would stop inhibiting the PDMS curing after several rounds of PDMS baking (usually 60 °C, minimum 2 hours).

### Combination of UV post-curing and thermal baking

For most VP resins, a single UV post-curing or thermal baking step is not enough to eliminate the leaching of curing inhibitors out of the moulds. This is why numerous post-treatments for VP (43 in Table 3) combine a first post-curing step with a thermal baking step. In total, 33 resins were





treated using UV post-curing, thermal baking, or a combination of both treatments, making such a protocol a legitimate candidate for a title of “universal” post-treatment for VP resins. Such a combination has one strong advantage: its accessibility. A UV curing box is often sold with 3D printers, and an oven or a hotplate is a classical piece of equipment in most labs.

### Mould surface coating

Coating the moulds with a protective layer that limits or suppresses the diffusion of inhibitors is also an efficient

strategy. In our database (Table 4), 23 different coatings are referenced; some of them aim at reducing the PDMS curing inhibition, especially when applied without any other post-treatments. The coating could also improve the surface roughness of the mould, simplifying the optical imaging through a moulded PDMS part, or the plasma bonding of PDMS on another substrate, when applied after UV post-curing or thermal baking. In more detail, silicone, ink and lacquer were applied by manual airbrushing, with thicknesses of up to 50 µm. Parylene has been applied by vacuum deposition, with a thickness down to 18 nm. Finally, high-tech, clean room processes have also been tested,

**Table 4** Post-treatments including coatings

Reference	Resin	UV post-curing	Thermal baking	Coating	
		Wavelength, dose, temperature	Duration, temperature	Material	Method
VAT photopolymerization					
Mohamed <sup>134</sup>	Formlabs, Clear GPCL02			Gold–palladium, 10 nm	Sputtering
Olanrewaju <sup>61</sup>	Envisiontec, HTM140			Silicone (ease release 200)	Spray
Escudero <sup>72</sup>	DWS, DL260			SiO <sub>2</sub> (15 nm), then PFDTCS monolayer	Surface preparation deposition (Memsstar)
Hagemann <sup>71</sup>	Anycubic, Clear	1 h, 405 nm		Enamel paint (Plastikote), <50 µm	Airbrushing
Hagemann <sup>71</sup>	Elegoo, ABS-like	1 h, 405 nm		Enamel paint (Plastikote), <50 µm	Airbrushing
Hagemann <sup>71</sup>	LiqCreate, Premium Tough	1 h, 405 nm		Enamel paint (Plastikote), <50 µm	Airbrushing
Hagemann <sup>71</sup>	Phrozen, Water washable model gray	1 h, 405 nm		Enamel paint (Plastikote), <50 µm	Airbrushing
O'Grady <sup>70</sup>	Formlabs, Grey	1 min, 405 nm, 5.5 mW cm <sup>-2</sup> , 60 °C		Parylene, 18 nm	Vacuum deposition
O'Grady <sup>70</sup>	Formlabs, Clear	1 min, 405 nm, 5.5 mW cm <sup>-2</sup> , 60 °C		Parylene, 18 nm	Vacuum deposition
Comina <sup>37</sup>	Miicraft, unspecified	10 min		Ink (Pentel NN60)	Airbrushing
Otroshchenko <sup>135</sup>	Eryone, White water washable	10 min, 405 nm	6 h, 100 °C	PTFE	Sputtering with O <sub>2</sub> or N <sub>2</sub> plasma
Otroshchenko <sup>135</sup>	Phrozen, TR250LV	10 min, 405 nm	6 h, 100 °C	PTFE	Sputtering with O <sub>2</sub> or N <sub>2</sub> plasma
Otroshchenko <sup>135</sup>	Resione, G217	10 min, 405 nm	6 h, 100 °C	PTFE	Sputtering with O <sub>2</sub> or N <sub>2</sub> plasma
Otroshchenko <sup>135</sup>	Resione, HT100	10 min, 405 nm	6 h, 100 °C	PTFE	Sputtering with O <sub>2</sub> or N <sub>2</sub> plasma
Byrne <sup>136</sup>	Formlabs, Clear	15 min, 405 nm, 5.5 mW cm <sup>-2</sup> , 60 °C	2 h, 130 °C	Lacquer thinner (Klean-Strip) and clear coat (Finish 1 FC720/FH612), 40 µm	Airbrushing
Byrne <sup>136</sup>	Formlabs, Grey	30 min, 405 nm, 5.5 mW cm <sup>-2</sup> , 60 °C	3 h, 130 °C	Lacquer thinner (Klean-Strip) and clear coat (Finish 1 FC720/FH612), 40 µm	Airbrushing
Dediu <sup>137</sup>	Creative CADWorks, Master Mold Resin	1 h, 405 nm	20 h, 65 °C	Aluminum, 300 nm	E-beam high vacuum thin film deposition
Yi <sup>138</sup>	Formlabs, High Temperature	4 h	1 h, 130 °C	Dry film lubricant (Electrolube)	Spray
Material jetting					
Guvanasen <sup>39</sup>	Objet, Transparent Fullcure 720			Gold (0.4 nm) and Knock Out Mold Release SU-82002	Sputtering and painting
Chande <sup>139</sup>	Stratasys, VeroBlack				Spin-coating, soft-bake, UV exposure
Hwang <sup>140</sup>	Stratasys, VeroWhitePlus			Platinum, 10 nm	Sputtering
Cairone <sup>141</sup>	Stratasys, VeroWhitePlus 835			Hydrosoluble acrylic acid polymers (Sokalan)	Drying on top of the mould
Hwang <sup>82</sup>	Stratasys VeroWhitePlus RGD835			Gold–palladium, 10 nm	Sputtering with different angles

PFDTCS: trichloro(1*H*,1*H*,2*H*,2*H*-perfluorodecyl)silane.



including aluminium, platinum, palladium and gold sputtering, SiO<sub>2</sub> coating, SU-8 spin-coating and plasma-based Teflon deposition. When choosing a coating, care has to be taken about the following parameters: price of the equipment, reproducibility of manual operation like airbrushing, comparison of the thickness of the coating and the smallest feature printed in the mould, and preferential adhesion of the coating on the mould compared to PDMS, to avoid transferring it to the replica.

### Silanization

Silanization is a specific type of coating which is often used with PDMS, glass or silicon in the microfluidics and microfabrication community, but has also been shown to be applicable to other substrates like metal or polymers. Usually, the substrate has first to be oxidized with a plasma treatment, and then a silane monolayer is formed by immersing the substrate in a silane-solvent solution or by vapour deposition. The silicon oxide part of the silane bonds to the oxidized substrate. In these post-treatment, the silanes used are perfluorosilane, adding a “Teflon-like” monolayer

on top of the polymerized resin. Such a treatment reduces the PDMS curing inhibition and the bonding of the silicone on the acrylate surface (see Table 5). For this second objective, silanization has been added to previously described post-treatments. It has also been a popular treatment to help the detachment of PDMS replicas on 2PP moulds. The mechanism of the functionalization of acrylates by silane has not been studied. Is it classical grafting after plasma oxidation? Simply adsorption? One attention point: as being part of the eternal pollutant category, the use of fluorosilane might be restricted in the future. Fortunately, many alternatives to silanization are available for treatment of 3D-printed moulds.

### Immersion in solvents

As inhibition of PDMS curing is due to molecules leaching out of the 3D-printed moulds, another strategy is to promote such leaching before the PDMS moulding by immersing the moulds in solvents. For aqueous solutions, numerous studies have reported the leaching of various molecules, mostly when studying the cytotoxicity of 3D-printed leachates for cells or

**Table 5** Post-treatments including silanization

Reference	Resin	UV post-curing	Thermal baking	Silanization	
		Wavelength, dose, temperature	Duration, temperature	Plasma activation	Coating
VAT photopolymerization					
Zhang <sup>142</sup>	Anycubic, unspecified			No	Immersion for 2 h in 1% wt PFOTES-ethanol
Liu <sup>143</sup>	Anycubic, unspecified	60 min	2 h, 120 °C	3 min	Spin-coating of PFOTCS
Credi <sup>144</sup>	DWS, DL260	15 min, 2.1 mW cm <sup>-2</sup> at 405 nm	1 h, 100 °C	Air plasma, 150 W, 60 s	Immersion for 1 h in 1% PFDTES-toluene
Vedhanayagam <sup>52</sup>	Phrozen, Aqua Grey 8K	30 min	1 h, 60 °C	No	Vapour deposition of PFOTCS for 25 min under vacuum
Han <sup>30</sup>	Asiga, PlasCLEAR	3 min (Asiga UV chamber)	1 h, 120 °C, autoclave	Oxygen plasma, 1 min	Vapour deposition of PFOTCS for 2 h under vacuum
Chan <sup>84</sup>	Miicraft, unspecified	10 min	4 h, 130 °C	Oxygen plasma, 3 min	Vapour deposition of PFOTCS for 30 min under vacuum
Wang <sup>145</sup>	Asiga, PlasCLEAR v2.0	30 min	48 h, 70 °C	No	Vapour deposition of PFOTCS for 2 h under vacuum
Material jetting					
King <sup>38</sup>	Stratasys, VeroClear		24 h, 80 °C	No	Vapour deposition of PFOTCS for 1 h under vacuum
King <sup>38</sup>	Stratasys, VeroGrey		24 h, 80 °C	No	Vapour deposition of PFOTCS for 1 h under vacuum
King <sup>38</sup>	Stratasys, VeroWhite Plus		24 h, 80 °C	No	Vapour deposition of PFOTCS for 1 h under vacuum
Glick <sup>41</sup>	3D Systems, VisiJet EX200		45 min, 75 °C, then 1 h, 80 °C	No	Vapour deposition of PFOTCS for 30 min under vacuum
Kim <sup>146</sup>	3D Systems, VisiJet M2S-HT90		24 h, 80 °C	Oxygen plasma, 1 min, 100 W, 1.2 Torr	Vapour deposition of PFOTCS for 2 h under vacuum and at 70 °C
Two-photon polymerization					
Koppaka <sup>63</sup>	Nanoscribe, IP-S		5 min, 190 °C	No	Vapour deposition of PFOTCS for 45 min
Jiménez-Díaz <sup>147</sup>	Nanoscribe, IP-S			No	Vapour deposition of PFOCTS for 2 h under vacuum
Huang <sup>74</sup>	Nanoscribe, IP-S			No	Silanization with PFOTCS

PFOTCS: trichloro(1*H*,1*H*,2*H*,2*H*-perfluorooctyl)silane. PFOTES: 1*H*,1*H*,2*H*,2*H*-perfluorooctyltriethoxysilane. PFDTES: 1*H*,1*H*,2*H*,2*H*-perfluorodecyltriethoxysilane.

PFOTES: 1*H*,1*H*,2*H*,2*H*-perfluorooctyltriethoxysilane. PFDTES: 1*H*,1*H*,2*H*,2*H*-perfluorodecyltriethoxysilane.



**Table 6** Post-treatments including immersion in solvents

		UV post-curing				Silanization	
Reference	Resin	Duration	Wavelength	Dose	Solvent	Plasma	Silane
VAT photopolymerization Tjong <sup>152</sup>	B9Creations, B9-R2-Black	20 min	X	X	2 × 24 h in isopropanol or ethanol		
Costa <sup>53</sup>	Envisiontec, PIC100	3500 flashes	280–700 nm	200 W per flash	7 h in ethanol at 37 °C, bath change every 2 h		
Li <sup>59</sup>	Anycubic, unspecified	20 min	X	X	6 h in isopropanol	Air plasma corona, 1 min	PFOTES for 3 h
Waheed <sup>153</sup>	Miicraft, BV003	5 min	315–400 nm	X	6 h in isopropanol	Air plasma corona, 1 min	PFOTES for 3 h under vacuum
Shrestha <sup>77</sup>	Miicraft, BV007	3 min	X	X	2 h in ethanol	Oxygen plasma, 2 min	PFOTCS for 90 min under vacuum
Reference	Resin	Solvent			Thermal baking	Solvent	
VAT photopolymerization Woo <sup>154</sup>	Formlabs, Clear RS-F2-GPCL-04	2 h in de-ionized water			18 h at 90 °C in a vacuum oven	1 h in de-ionized water with 0.1% Tween-20	
Franko <sup>155</sup>	Anycubic Clear	15 min in isopropanol			1 h at 100 °C	15 min in isopropanol	
Reference	Resin	Solvent			Coating		
VAT photopolymerization Zhang <sup>156</sup>	Shenzhen small sample, 150S	4 h in ethanol			Spraying of Ease Release 200		
		UV post-curing				Thermal	
Reference	Resin	Duration	Wavelength	Dose	Solvent	baking	
Material jetting Tabesh <sup>64</sup>	Stratasys, unspecified	10 min	405 nm	14 W cm <sup>−2</sup>	2 h in isopropanol + ultrasound	24 h, 80 °C	
X corresponds to data unavailable in the references. PFOTCS: trichloro(1 <i>H</i> ,1 <i>H</i> ,2 <i>H</i> ,2 <i>H</i> -perfluorooctyl)silane. PFOTES: 1 <i>H</i> ,1 <i>H</i> ,2 <i>H</i> ,2 <i>H</i> -perfluorooctyltriethoxysilane.							

X corresponds to data unavailable in the references. PFOTCS: trichloro(1*H*,1*H*,2*H*,2*H*-perfluorooctyl)silane. PFOTES: 1*H*,1*H*,2*H*,2*H*-perfluorooctyltriethoxysilane.

organisms. In particular, the following molecules have been detected: polyethylene glycol, diethyl phthalate,<sup>148</sup> (meth)acrylate monomers,<sup>149</sup> photo-initiators,<sup>150</sup> diphenyl sulphide, dicumyl peroxide, and benzoic acid ester.<sup>151</sup> However, PDMS is highly hydrophobic and then molecules leaching to PDMS are more prone to be extracted by a non-polar solvent compared to aqueous solutions. Even if immersion in solvent seems to be a simple step to apply at first, this step alone is not efficient enough to reduce PDMS inhibition and has to be combined with UV post-curing, thermal baking and/or silanization (see Table 6). The reason behind such inefficiency seems to be related to the low solubility of acrylate monomers and photo-initiators in the solvents used (ethanol, isopropanol and water), while better solvents would quite surely swell, crack and deform the printed moulds.

### Advices about this post-treatment database

This review aims at proposing enough post-treatment options to facilitate the use of 3D printed moulds for soft lithography. However, one should take care of several points when replicating the proposed protocols:

- Post-treatment efficiency, especially for volume-based treatments (thermal baking, UV post-curing, immersion in solvents), depends strongly on the design, shape and volume of the moulds. In particular, reducing the thickness of the

base should reduce the duration of the treatments as the quantity of leachates is reduced.

- Warping and bending of moulds are usual problems, which are rarely reported in the final manuscripts. One of the main reasons in VP is the printing of the mould directly on the print platform, with the first layers being overcured to increase the adhesion of the print. This overcuring leads to differential shrinkage of the different layers and bending of the mould. This could be avoided by adding a base and breakable pillars below the mould, and by reinforcing the

**Table 7** Resins with no post-treatment found or needed

Reference	Resin	Post-treatment
VAT photopolymerization		
Hagemann <sup>71</sup>	Phrozen, LiqCreate Flexible X	No treatment found
Hwang <sup>140</sup>	3D Systems, Accura 60	No treatment needed
Hwang <sup>140</sup>	ZR80	No treatment needed
Material jetting		
Hwang <sup>140</sup>	3D Systems, VisiJet Crystal	No treatment needed
Two-photon polymerization		
Koroleva <sup>42</sup>	Envisiontec, E-shell 300	No treatment needed
Hu <sup>49</sup>	SU8-25	No treatment needed
Soffe <sup>73</sup>	Microchip, IP-PH	No treatment needed
Barata <sup>164</sup>	Nanoscribe, IP-L	No treatment needed
Lamont <sup>62</sup>	Nanoscribe, IP-S	No treatment needed
Ugrinic <sup>60</sup>	Nanoscribe, IP-Q	No treatment needed
Hirschwald <sup>165</sup>	Nanoscribe, IP-S	No treatment needed
Kluck <sup>17</sup>	UpNano, UpBrix	No treatment needed





mould with large walls around the design, which could also serve as a reservoir for the PDMS.

- Formulations of commercial resins are sometimes modified without changing the name of the resin. A good example is Formlabs Clear (going from version 1 to version 4) or High Temperature, where the version 2 needs a completely different post-treatment than the version 1.

- Soft lithography has been shown to replicate even nanoscale details.<sup>7</sup> Therefore, except when the curing is partially inhibited, all details of the moulds should be replicated. No reports of modification of the mould resolution by post-treatment have been found, but care has to be taken with coating based protocols that might add a significant thickness.

Taking into account these precautions and checking the updated database for more protocols would help the microfluidic community strongly in searching for a simple technique to fabricate moulds for soft lithography.

## Conclusions and perspectives on post-treatments

Post-treatments were found for a large number of resins. Only one resin could not be turned PDMS-compatible, while only two VP, one MJ and seven 2PP resins did not need any post-treatments (Table 7). Resins sold as medical grade were the easiest ones to treat (for example Formlabs BioMed or DWS DS3000), while flexible/elastic resins were particularly difficult to treat (Formlabs Elastic, LiqCreate Flexible X or DWS GL4000). It is interesting to note that biocompatible resins require short post-treatments, meaning that they leach the smallest amount of toxic components, both for the PDMS catalyst and for animal cells. Looking at the literature about post-treatments for biocompatibility of 3D-printed structures, and in particular 3D printed chips, the same types of treatments are used to render chips biocompatible: UV post-curing,<sup>149,157</sup> incubation in water,<sup>158</sup> incubation in solvents,<sup>159,160</sup> autoclaving or baking,<sup>157,161,162</sup> and coating.<sup>70,161,163</sup> While we recognized that cell toxicity and PDMS inhibition might be caused by different molecules, at different concentrations, the proposed database of post-treatments for soft lithography could also be a useful tool to design post-treatment for biocompatibility, as well as selecting resins which should be the least toxic for cell culture experiments in 3D-printed chips.

## Data availability

The data supporting this article have been included as part of the ESI.† The post-treatment database is available as an .xlsx document at Zenodo at <https://doi.org/10.5281/zenodo.13881893>.

## Conflicts of interest

There are no conflicts to declare.

## Acknowledgements

The author would like to thank Séverine Le Gac and Matic Može for the communication of unpublished post-treatment protocols. This work has been funded by the French National Research Agency (ANR) by the grant ANR-23-CE19-0004-01.

## References

- 1 F. Schneider, J. Draheim, R. Kamberger and U. Wallrabe, *Sens. Actuators, A*, 2009, **151**, 95–99.
- 2 K. Khanafer, A. Duprey, M. Schlicht and R. Berguer, *Biomed. Microdevices*, 2009, **11**, 503–508.
- 3 G. Firpo, E. Angeli, L. Repetto and U. Valbusa, *J. Membr. Sci.*, 2015, **481**, 1–8.
- 4 S. G. Charati and S. A. Stern, *Macromolecules*, 1998, **31**, 5529–5535.
- 5 G. G. Morbioli, N. C. Speller and A. M. Stockton, *Anal. Chim. Acta*, 2020, **1135**, 150–174.
- 6 T. Fujii, *Microelectron. Eng.*, 2002, **61–62**, 907–914.
- 7 X.-M. Zhao, Y. Xia and G. M. Whitesides, *J. Mater. Chem.*, 1997, **7**, 1069–1074.
- 8 S. W. Lee and S. S. Lee, *Microsyst. Technol.*, 2007, **14**, 205–208.
- 9 M. A. Eddings, M. A. Johnson and B. K. Gale, *J. Micromech. Microeng.*, 2008, **18**, 067001.
- 10 J. N. Lee, C. Park and G. M. Whitesides, *Anal. Chem.*, 2003, **75**, 6544–6554.
- 11 B. J. van Meer, H. de Vries, K. S. A. Firth, J. van Weerd, L. G. J. Tertoolen, H. B. J. Karperien, P. Jonkheijm, C. Denning, A. P. IJzerman and C. L. Mummery, *Biochem. Biophys. Res. Commun.*, 2017, **482**, 323–328.
- 12 M. W. Toepke and D. J. Beebe, *Lab Chip*, 2006, **6**, 1484–1486.
- 13 D. T. Eddington, J. P. Puccinelli and D. J. Beebe, *Sens. Actuators, B*, 2006, **114**, 170–172.
- 14 H. Becker, *Lab Chip*, 2010, **10**, 271–273.
- 15 E. Berthier, E. W. K. Young and D. Beebe, *Lab Chip*, 2012, **12**, 1224.
- 16 Z. Faraji Rad, P. D. Prewett and G. J. Davies, *Manuf. Lett.*, 2021, **30**, 39–43.
- 17 S. Kluck, R. Prediger, L. Hambitzer, N. Nekoonam, F. Dreher, M. Luitz, M. Lunzer, M. Worgull, M. Schneider, B. E. Rapp and F. Kotz-Helmer, *Adv. Sci.*, 2024, **11**, 2405320.
- 18 D. C. Duffy, J. C. McDonald, O. J. A. Schueller and G. M. Whitesides, *Anal. Chem.*, 1998, **70**, 4974–4984.
- 19 M. E. Wilson, N. Kota, Y. Kim, Y. Wang, D. B. Stolz, P. R. LeDuc and O. Burak Ozdoganlar, *Lab Chip*, 2011, **11**, 1550–1555.
- 20 G. Pitingolo, V. Taly and C. Nestruzzi, *Biomechanics*, 2019, **13**, 024106.
- 21 W. Wu, R. M. Guijt, Y. E. Silina, M. Koch and A. Manz, *RSC Adv.*, 2016, **6**, 22469–22475.
- 22 J. C. McDonald, M. L. Chabinyc, S. J. Metallo, J. R. Anderson, A. D. Stroock and G. M. Whitesides, *Anal. Chem.*, 2002, **74**, 1537–1545.



- 23 N. P. Macdonald, J. M. Cabot, P. Smejkal, R. M. Guijt, B. Paull and M. C. Breadmore, *Anal. Chem.*, 2017, **89**, 3858–3866.
- 24 A. Accardo, R. Courson, R. Riesco, V. Raimbault and L. Malaquin, *Addit. Manuf.*, 2018, **22**, 440–446.
- 25 H. Gong, B. P. Bickham, A. T. Woolley and G. P. Nordin, *Lab Chip*, 2017, **17**, 2899–2909.
- 26 C. Vidler, K. Crozier and D. Collins, *Microsyst. Nanoeng.*, 2023, **9**, 1–13.
- 27 A. Amini, R. M. Guijt, T. Themelis, J. De Vos and S. Eeltink, *J. Chromatogr. A*, 2023, **1692**, 463842.
- 28 H. Shafique, V. Karamzadeh, G. Kim, M. L. Shen, Y. Morocz, A. Sohrabi-Kashani and D. Juncker, *Lab Chip*, 2024, **24**, 2774–2790.
- 29 M. Ramasamy, B. Ho, C.-M. Phan, N. Qin, C. L. Ren and L. Jones, *J. Micromech. Microeng.*, 2023, **33**, 105016.
- 30 D. H. Han, U. Oh and J.-K. Park, *ACS Omega*, 2023, **8**, 19128–19136.
- 31 M. Dewaele, D. Truffier-Boutry, J. Devaux and G. Leloup, *Dent. Mater.*, 2006, **22**, 359–365.
- 32 H. K. Balakrishnan, F. Badar, E. H. Doeven, J. I. Novak, A. Merenda, L. F. Dumée, J. Loy and R. M. Guijt, *Anal. Chem.*, 2021, **93**, 350–366.
- 33 Y. Liu, G. Jin, J.-H. Lim and J.-E. Kim, *Sci. Rep.*, 2024, **14**, 9909.
- 34 A. Garg, S. S. Yerneni, P. Campbell, P. R. LeDuc and O. B. Ozdoganlar, *Adv. Sci.*, 2022, **9**, 2201566.
- 35 S. C. Ligon, R. Liska, J. Stampfl, M. Gurr and R. Mülhaupt, *Chem. Rev.*, 2017, **117**, 10212–10290.
- 36 A. Elkaseer, K. J. Chen, J. C. Janhsen, O. Refle, V. Hagenmeyer and S. G. Scholz, *Addit. Manuf.*, 2022, **60**, 103270.
- 37 G. Comina, A. Suska, D. Filippini, A. S. German Comina and D. Filippini, *Lab Chip*, 2013, **14**, 424–430.
- 38 P. H. King, G. Jones, H. Morgan, M. R. R. de Planque and K.-P. Zauner, *Lab Chip*, 2014, **14**, 722–729.
- 39 G. S. Guvanasen, M. L. Mancini, W. A. Calhoun, S. Rajaraman and S. P. DeWeerth, *J. Microelectromech. Syst.*, 2014, **23**, 1045–1053.
- 40 Y. Hwang, O. H. Paydar and R. N. Candler, *Sens. Actuators, A*, 2015, **226**, 137–142.
- 41 C. C. Glick, M. T. Srimongkol, A. J. Schwartz, W. S. Zhuang, J. C. Lin, R. H. Warren, D. R. Tekell, P. A. Satamalee and L. Lin, *Microsyst. Nanoeng.*, 2016, **2**, 1–9.
- 42 A. Koroleva, S. Gittard, S. Schlie, A. Deiwick, S. Jockenhoevel and B. Chichkov, *Biofabrication*, 2012, **4**, 015001.
- 43 M. Pawlicki, H. A. Collins, R. G. Denning and H. L. Anderson, *Angew. Chem., Int. Ed.*, 2009, **48**, 3244–3266.
- 44 F. Cantoni, D. Maher, E. Bosler, S. Kühne, L. Barbe, D. Oberschmidt, C. Marquette, R. Taboryski, M. Tenje and A.-I. Bunea, *Addit. Manuf.*, 2023, **76**, 103761.
- 45 J. Bauer, A. G. Izard, Y. Zhang, T. Baldacchini and L. Valdevit, *Adv. Mater. Technol.*, 2019, **4**, 1900146.
- 46 A. Sharaf, J. P. Frimat, G.-J. Kremers and A. Accardo, *Micro Nano Eng.*, 2023, 100188.
- 47 M. Stoneman, M. Fox, C. Zeng and V. Raicu, *Lab Chip*, 2009, **9**, 819–827.
- 48 Y. Xia, C. Song, Y. Meng, P. Xue, A. J. deMello, Q. Gao, S. Stavrakis, S. Ma and X. Cao, *Sens. Actuators, B*, 2022, **369**, 132276.
- 49 C. Hu, J. Kearn, P. Urwin, C. Lilley, V. O. Connor, L. Holden-Dye and H. Morgan, *Lab Chip*, 2014, **14**, 2447–2455.
- 50 J. Tang, G. Qiu, X. Cao, Y. Yue, X. Zhang, J. Schmitt and J. Wang, *Lab Chip*, 2020, **20**, 2334–2342.
- 51 J. Purtov, A. Verch, P. Rogin and R. Hensel, *Microelectron. Eng.*, 2018, **194**, 45–50.
- 52 A. Vedhanayagam, M. Golfetto, J. L. Ram and A. S. Basu, *Micromachines*, 2023, **14**, 1519.
- 53 P. F. Costa, H. J. Albers, J. E. A. Linssen, H. H. T. Middelkamp, L. van der Hout, R. Passier, A. van den Berg, J. Malda and A. D. van der Meer, *Lab Chip*, 2017, **17**, 2785–2792.
- 54 S. Sharma, B. Venzac, T. Burgers, S. Schlatt and S. Le Gac, *Organs-on-a-Chip*, 2022, **4**, 100023.
- 55 K. Stephan, P. Pittet, L. Renaud, P. Kleimann, P. Morin, N. Ouaini and R. Ferrigno, *J. Micromech. Microeng.*, 2007, **17**, N69–N74.
- 56 R. M. Guijt and M. C. Breadmore, *Lab Chip*, 2008, **8**, 1402.
- 57 S. Razavi Bazaz, N. Kashaninejad, S. Azadi, K. Patel, M. Asadnia, D. Jin and M. Ebrahimi Warkiani, *Adv. Mater. Technol.*, 2019, **4**, 1900425.
- 58 E. Sharma, R. Rath, J. Misharwal, B. Sinhar, S. Kumari, J. Dalal and A. Kumar, *Nanomaterials*, 2022, **12**, 2754.
- 59 Y. Li, J. E. Sanfilippo, D. Kearns and J. Q. Yang, *Microbiol. Spectrum*, 2022, **10**(5), e03233–22.
- 60 M. Ugrinic, D. Decanini, N. Bidan, G. Lazzari, A. Harouri, G. Hwang, A.-M. Haghiri-Gosnet and S. Mura, *Microelectron. Eng.*, 2023, **267–268**, 111898.
- 61 A. O. Olanrewaju, A. Robillard, M. Dagher and D. Juncker, *Lab Chip*, 2016, **16**, 3804–3814.
- 62 A. C. Lamont, A. T. Alsharhan and R. D. Sochol, *Sci. Rep.*, 2019, **9**, 394.
- 63 S. Koppaka, K. S. Zhang, M. Kurosu Jalil, L. R. Blauch and S. K. Y. Tang, *Micromachines*, 2021, **12**, 1005.
- 64 E. Tabesh, S. N. Leung and P. Rezai, *Mater. Today Commun.*, 2023, **35**, 106369.
- 65 M. Wu, S. Wu, G. Wang, W. Liu, L. T. Chu, T. Jiang, H. K. Kwong, H. L. Chow, I. W. S. Li and T.-H. Chen, *Sci. Adv.*, 2022, **8**, eabn6064.
- 66 S. Ye, W.-C. Chin and C.-W. Ni, *Biomed. Microdevices*, 2023, **25**, 30.
- 67 Y.-J. Chang, K. Mohseni and V. M. Bright, *Sens. Actuators, A*, 2007, **136**, 546–553.
- 68 M. Gaudet and S. Arscott, *Anal. Methods*, 2017, **9**, 2495–2504.
- 69 L.-Y. Liu, L.-Y. Liu and Y.-C. Su, *Sens. Actuators, A*, 2023, **354**, 114230.
- 70 B. J. O'Grady, M. D. Geuy, H. Kim, K. M. Balotin, E. R. Allchin, D. C. Florian, N. N. Bute, T. E. Scott, G. B. Lowen, C. M. Fricker, M. L. Fitzgerald, S. A. Guelcher, J. P. Wikswo,



- L. M. Bellan and E. S. Lippmann, *Lab Chip*, 2021, **21**, 4814–4822.
- 71 C. Hagemann, M. C. D. Bailey, E. Carraro, K. S. Stankevich, V. M. Lionello, N. Khokhar, P. Suklai, C. Moreno-Gonzalez, K. O'Toole, G. Konstantinou, C. L. Dix, S. Joshi, E. Giagnorio, M. S. Bergholt, C. D. Spicer, A. Imbert, F. S. Tedesco and A. Serio, *PLoS Biol.*, 2024, **22**, e3002503.
  - 72 M. Escudero, L. Vaysse, G. Eke, M. Peyrou, F. Villarroya, S. Bonnel, Y. Jeanson, L. Boyer, C. View, B. Chaput, X. Yao, F. Deschaseaux, M. Parny, I. Raymond-Letron, C. Dani, A. Carrière, L. Malaquin and L. Casteilla, *Adv. Sci.*, 2023, **10**, 2301499.
  - 73 R. Soffe, S. Baratchi, M. Nasabi, S.-Y. Tang, A. Boes, P. McIntyre, A. Mitchell and K. Khoshmanesh, *Sens. Actuators, B*, 2017, **251**, 963–975.
  - 74 C. Huang, J. A. Wippold, D. Stratis-Cullum and A. Han, *Biomed. Microdevices*, 2020, **22**, 76.
  - 75 M. A. Unger, H. P. Chou, T. Thorsen, A. Scherer and S. R. Quake, *Science*, 2000, **288**, 113–116.
  - 76 D. Huh, B. D. Matthews, A. Mammoto, M. Montoya-Zavala, H. Y. Hsin and D. E. Ingber, *Science*, 2010, **328**, 1662–1668.
  - 77 J. Shrestha, M. Ghadiri, M. Shanmugavel, S. Razavi Bazaz, S. Vasilescu, L. Ding and M. Ebrahimi Warkiani, *Organs-on-a-Chip*, 2019, **1**, 100001.
  - 78 M. de Almeida Monteiro Melo Ferraz, J. B. Nagashima, B. Venzac, S. Le Gac and N. Songsasen, *Sci. Rep.*, 2020, **10**, 1575.
  - 79 T. C. Cameron, A. Randhawa, S. M. Grist, T. Bennet, J. Hua, L. G. Alde, T. M. Caffrey, C. L. Wellington and K. C. Cheung, *Micromachines*, 2022, **13**, 1573.
  - 80 M. K. S. Verma, A. Majumder and A. Ghatak, *Langmuir*, 2006, **22**, 10291–10295.
  - 81 A. Asthana, K.-O. Kim, J. Perumal, D.-M. Kim and D.-P. Kim, *Lab Chip*, 2009, **9**, 1138–1142.
  - 82 Y. Hwang, O. H. Paydar and R. N. Candler, *Sens. Actuators, A*, 2015, **234**, 65–71.
  - 83 S. Karam, N. Shirdade, B. Madden, J. Rheinstadter, E. W. Church, M. C. Brindise and G. Manogharan, *Manuf. Lett.*, 2023, **35**, 770–777.
  - 84 H. N. Chan, Y. Chen, Y. Shu, Y. Chen, Q. Tian and H. Wu, *Microfluid. Nanofluid.*, 2015, **19**, 9–18.
  - 85 H. Hinnen, M. Viglione, T. R. Munro, A. T. Woolley and G. P. Nordin, *Micromachines*, 2023, **14**, 1286.
  - 86 B. W. Caplins, C. I. Higgins, T. J. Kolibaba, U. Arp, C. C. Miller, D. L. Poster, C. J. Zarobila, Y. Zong and J. P. Killgore, *Addit. Manuf.*, 2023, **62**, 103381.
  - 87 F. Formanek, N. Takeyasu, T. Tanaka, K. Chiyoda, A. Ishikawa and S. Kawata, *Opt. Express*, 2006, **14**, 800–809.
  - 88 V. Hahn, T. Messer, N. M. Bojanowski, E. R. Curticean, I. Wacker, R. R. Schröder, E. Blasco and M. Wegener, *Nat. Photonics*, 2021, **15**, 932–938.
  - 89 V. Hahn, P. Rietz, F. Hermann, P. Müller, C. Barner-Kowollik, T. Schlöder, W. Wenzel, E. Blasco and M. Wegener, *Nat. Photonics*, 2022, **16**, 784–791.
  - 90 G. Vizsnyiczai, L. Kelemen and P. Ormos, *Opt. Express*, 2014, **22**, 24217–24223.
  - 91 A. Balena, M. Bianco, F. Pisanello and M. De Vittorio, *Adv. Funct. Mater.*, 2023, **33**, 2211773.
  - 92 B. E. Kelly, I. Bhattacharya, H. Heidari, M. Shusteff, C. M. Spadaccini and H. K. Taylor, *Science*, 2019, **363**, 1075–1079.
  - 93 M. Regehy, Y. Garmshausen, M. Reuter, N. F. König, E. Israel, D. P. Kelly, C.-Y. Chou, K. Koch, B. Asfari and S. Hecht, *Nature*, 2020, **588**, 620–624.
  - 94 G. L. Flowers and S. T. Switzer, *Background material properties of selected silicone potting compounds and raw materials for their substitutes*, Mason and Hanger-Silas Mason Co., Inc., Amarillo, Tex. (USA), 1978.
  - 95 Anycubic Resin User Manual & MSDS | ANYCUBIC 3D Printing, <https://store.anycubic.com/pages/resin-user-manual>, (accessed 18 March 2025).
  - 96 Eggshell-AMB SDS, [https://support.3dsystems.com/s/article/materials-figure-4-eggshell-amb-10?language=en\\_US](https://support.3dsystems.com/s/article/materials-figure-4-eggshell-amb-10?language=en_US), (accessed 18 March 2025).
  - 97 B9R1-Cherry SDS, <https://www.b9c.com/hubfs/SDS%20Sheets/sds-b9r1-cherry-ghs.pdf>.
  - 98 DWS DL260 SDS, [https://www.3dconsommables.fr/wp-content/uploads/2023/07/Fiche\\_technique\\_DWS\\_Precisa\\_DL260.pdf](https://www.3dconsommables.fr/wp-content/uploads/2023/07/Fiche_technique_DWS_Precisa_DL260.pdf).
  - 99 Elegoo Resin MSDS, <https://www.elegoo.com/blogs/3d-printing/elegoo-resin-sds>, (accessed 18 March 2025).
  - 100 Safety Data Sheets - ETEC, <https://etec.desktopmetal.com/safety-data-sheets/>, (accessed 18 March 2025).
  - 101 Formlabs Clear V4, <https://media.formlabs.com/m/2e4666e1dc86f854/original/-ENUS-Safety-Data-Sheet-Clear-V4-1-Resin.pdf>.
  - 102 Fun-To-Do Industrial Blend, [https://www.2engineers.com/wp-content/uploads/2014/11/MSDS-FTD-IB\\_UK\\_Oct.pdf](https://www.2engineers.com/wp-content/uploads/2014/11/MSDS-FTD-IB_UK_Oct.pdf).
  - 103 LiqCreate Premium Tough SDS, <https://3ddentalstore.fr/wp-content/uploads/2021/11/Safety-data-sheet-of-Liqcreate-Premium-Tough-CLP.pdf>.
  - 104 Phrozen Aqua Grey SDS, <https://phrozen3d.com/pages/document>, (accessed 18 March 2025).
  - 105 Resione SDS, <https://www.resione.com/pages/msds>, (accessed 18 March 2025).
  - 106 Material Safety Data Sheets | Stratasys Support Center, <https://support.stratasys.com/en/materials/sds?phrase=rgd835>, (accessed 18 March 2025).
  - 107 L. N. Lewis, J. Stein, R. E. Colborn, Y. Gao and J. Dong, *J. Organomet. Chem.*, 1996, **521**, 221–227.
  - 108 F. Faglioni, M. Blanco, W. A. Goddard and D. Saunders, *J. Phys. Chem. B*, 2002, **106**, 1714–1721.
  - 109 I. Kownacki, B. Marciniak, H. Steinberger, M. Kubicki, M. Hoffmann, A. Ziarko, K. Szubert, M. Majchrzak and S. Rubinsztajn, *Appl. Catal., A*, 2009, **362**, 106–114.
  - 110 J. Li, C. Niu, J. Peng, Y. Deng, G. Zhang, Y. Bai, C. Ma, W. Xiao and G. Lai, *Appl. Organomet. Chem.*, 2014, **28**, 454–460.
  - 111 B. Venzac, S. Deng, Z. Mahmoud, A. Lenferink, A. Costa, F. Bray, C. Otto, C. Rolando and S. Le Gac, *Anal. Chem.*, 2021, **93**, 7180–7187.
  - 112 E. Grigorov, B. Kirov and V. Galabov, *A Combination of UV curing and thermal Treatment successfully overcomes PDMS*





- Curing Inhibition on 3D-Printed low-cost-resin Molds*, In Review, 2022.
- 113 J. D. Lundquist, L. Linkous, U. Hasni and E. Topsakal, *IEEE Open J. Antennas Propag.*, 2023, **4**, 434–445.
  - 114 J. Vogt and K. Rosenthal, *Sci*, 2022, **4**, 36.
  - 115 D. Som Yang, Y. Wu, E. E. Kanatzidis, R. Avila, M. Zhou, Y. Bai, S. Chen, Y. Sekine, J. Kim, Y. Deng, H. Guo, Y. Zhang, R. Ghaffari, Y. Huang and J. A. Rogers, *Mater. Horiz.*, 2023, **10**, 4992–5003.
  - 116 E. Cutuli, D. Sanalitro, G. Stella, L. Saitta and M. Bucolo, *Micromachines*, 2023, **14**, 2115.
  - 117 Y. Kang, J. Lee, S. Park, J. Kim, S. I. Kim and W. Ryu, *ACS Appl. Mater. Interfaces*, 2023, **15**, 17653–17663.
  - 118 R. Sanchez, M. Groc, R. Vuillemin, M. Pujo-Pay and V. Raimbault, *Sensors*, 1897, 2023, **23**.
  - 119 E. Stolovicki, R. Ziblat and D. A. Weitz, *Lab Chip*, 2018, **18**, 132–138.
  - 120 M. Cicolini, M. Cocuzza, G. Ciardelli, S. L. Marasso and C. Tonda Turo, *Development of a microfluidic alveolus-on-chip supporting epithelial-endothelial cells co-culture and air-liquid interface implementation for the modelling of the physiological alveolar-capillary barrier*, 2022.
  - 121 M. Segantini, M. Parmeggiani, A. Ballesio, G. Palmara, F. Frascella, S. L. Marasso and M. Cocuzza, *Sensors*, 2022, **22**, 969.
  - 122 G. Mossotti, A. Piscitelli, F. Catania, M. Aronne, G. Galfré, A. Lamberti, S. Ferrero, L. Scaltrito and V. Bertana, *Water*, 2024, **16**, 1167.
  - 123 T. Dinh, H.-P. Phan, N. Kashaninejad, T.-K. Nguyen, D. V. Dao and N.-T. Nguyen, *Adv. Mater. Interfaces*, 2018, **5**, 1800764.
  - 124 A. Jóskowiak, C. L. Nogueira, S. P. Costa, A. P. Cunha, P. P. Freitas and C. M. Carvalho, *Microchim. Acta*, 2023, **190**, 356.
  - 125 J. Lee, H. M. Cuong, J. Kim, E. Choi, H. Kee, S. Yang, J.-O. Park and S. Park, in *2023 IEEE/RSJ International Conference on Intelligent Robots and Systems (IROS)*, 2023, pp. 2628–2634.
  - 126 F. L. Memarian, D. A. Khaladj, D. Hammar and L. S. Hirst, *J. Visualized Exp.*, 2023, **191**, e64287.
  - 127 Y. Ö. Yilmaz, B. Venzac and S. Le Gac, *Final report: Assessing the properties of 10 different 3D printing resins on PDMS inhibition*, Twente University, 2022.
  - 128 X. Yang, T. Wu, D. Liu, J. Wu, Y. Wang, Y. Lu, Z. Ji, X. Jia, P. Jiang and X. Wang, *Addit. Manuf.*, 2023, **71**, 103580.
  - 129 S. Hu, H. Li, W. Lu, T. Han, Y. Xu, X. Shi, Z. Peng and X. Cao, *Adv. Funct. Mater.*, 2023, **34**, 2313458.
  - 130 M.-Y. Lee, H.-W. Yoon, S.-I. Kim, J.-S. Kwon and S.-J. Shin, *Biofabrication*, 2024, **16**, 045027.
  - 131 H. Khoo, W. S. Allen, N. Arroyo-Currás and S. C. Hur, *Sci. Rep.*, 2024, **14**, 17646.
  - 132 P.-C. Chen and J. Lawrensen, *Sens. Actuators, A*, 2024, **367**, 115080.
  - 133 C. E. Byrne, A. T. Martier, G. W. Kpeli, K. M. Conrad, W. Bralower, E. Olsen, G. Fortes, C. C. Culp, M. Wendell, K. A. Boone, M. R. Burow and M. J. Mondrinos, *Biotechnol. J.*, 2024, **19**, e202400550.
  - 134 M. G. A. Mohamed, H. Kumar, Z. Wang, N. Martin, B. Mills and K. Kim, *J. Manuf. Mater. Process.*, 2019, **3**, 26.
  - 135 A. Otroshchenko and M. V. Zyuzin, *Phys. Fluids*, 2022, **34**, 112015.
  - 136 C. E. Byrne, K. M. Conrad, A. T. Martier, G. Fortes, G. W. Kpeli, E. Olsen, W. Bralower, C. C. Culp, M. Wendell, K. A. Boone and M. J. Mondrinos, *bioRxiv*, 2023, preprint, DOI: [10.1101/2023.12.06.570409](https://doi.org/10.1101/2023.12.06.570409).
  - 137 V. Dediu, M. Carp, F. S. Iliescu, E. A. Laszlo, C. Pachiou and C. Iliescu, in *2022 International Semiconductor Conference (CAS)*, 2022, pp. 243–246.
  - 138 J. Yi, W. Haouas, M. Gauthier and K. Rabenorosoa, *Adv. Intell. Syst.*, 2024, 2400394.
  - 139 C. Chande, N. Riaz, V. Harbour, H. Noor, M. Torralba, Y.-H. Cheng, Z. Li, A. Tong, R. Voronov and S. Basuray, *Technology*, 2020, **08**, 50–57.
  - 140 Y. Hwang, D. Seo, M. Roy, E. Han, R. N. Candler and S. Seo, *J. Microelectromech. Syst.*, 2016, **25**, 238–240.
  - 141 F. Cairone, S. Gagliano, D. C. Carbone, G. Recca and M. Bucolo, *Microfluid. Nanofluid.*, 2016, **20**, 61.
  - 142 L. Zhang, W. Li, L. Wei, Y. Zhao, Y. Qiu, H. Liu, C. Huang and J. Huang, *Langmuir*, 2023, **39**, 13932–13945.
  - 143 X. Liu, M. Li, J. Zheng, X. Zhang, J. Zeng, Y. Liao, J. Chen, J. Yang, X. Zheng and N. Hu, *Micromachines*, 2022, **13**, 1479.
  - 144 C. Credi, D. Pintossi, C. L. Bianchi, M. Levi, G. Griffini and S. Turri, *Mater. Des.*, 2017, **133**, 143–153.
  - 145 Z. Wang, L. J. Y. Ong, Y. Gan, J.-M. Pereira, J. Zhang, S. Kasetsirikul, Y.-C. Toh and E. Sauret, *Lab Chip*, 2024, **24**, 4050–4059.
  - 146 S. Kim, S. K. Lee, A. Son, J.-H. Lee and H. G. Kim, *Adv. Healthcare Mater.*, 2023, **12**, 2301673.
  - 147 E. Jiménez-Díaz, M. Cano-Jorge, D. Zamarrón-Hernández, L. Cabriales, F. Pérez-Larios, A. Cruz-Ramírez, G. Vázquez-Victorio, T. Fiordelisio and M. Hautefeuille, *Micromachines*, 2019, **10**, 576.
  - 148 M. de Almeida Monteiro Melo Ferraz, H. H. W. Henning, P. Ferreira da Costa, J. Malda, S. Le Gac, F. Bray, M. B. M. van Duursen, J. F. Brouwers, C. H. A. van de Lest, I. Bertijn, L. Kraneburg, P. L. A. M. Vos, T. A. E. Stout and B. M. Gadella, *Environ. Sci. Technol. Lett.*, 2018, **5**, 80–85.
  - 149 S. M. Oskui, G. Diamante, C. Liao, W. Shi, J. Gan, D. Schlenk and W. H. Grover, *Environ. Sci. Technol. Lett.*, 2016, **3**, 1–6.
  - 150 M. Carve and D. Wlodkowic, *Micromachines*, 2018, **9**, 91.
  - 151 M. Walpitagama, M. Carve, A. M. Douek, C. Trestrail, Y. Bai, J. Kaslin and D. Wlodkowic, *Aquat. Toxicol.*, 2019, **213**, 105227.
  - 152 J. Tjong, A. Teixeira and F. John, Solvent Extraction of 3D Printed Molds for Soft Lithography – Chips and Tips, <https://blogs.rsc.org/chipsandtips/2020/06/12/solvent-extraction-of-3d-printed-molds-for-soft-lithography/>, (accessed 29 November 2022).
  - 153 S. Waheed, J. M. Cabot, N. P. Macdonald, U. Kalsoom, S. Farajikhah, P. C. Innis, P. N. Nesterenko, T. W. Lewis, M. C. Breadmore and B. Paull, *Sci. Rep.*, 2017, **7**, 15109.
  - 154 S. O. Woo, M. Oh and Y. Choi, *STAR Protoc.*, 2022, **3**, 101376.



- 155 R. Franko and M. de A. M. M. Ferraz, *Lab Chip*, 2025, **25**, 187–200.
- 156 X. Zhang, Y. Liu, Y. Bao, Z. Zheng, J. Mi, Y. Tang, Q. Zhang and A. E. Oseyemi, *Microchim. Acta*, 2024, **191**, 583.
- 157 I. Salmon, S. Grebenyuk, A. R. A. Fattah, G. Rustandi, T. Pilkington, C. Verfaillie and A. Ranga, *Lab Chip*, 2022, **22**, 1615–1629.
- 158 G. González, D. Baruffaldi, C. Martinengo, A. Angelini, A. Chiappone, I. Roppolo, C. F. Pirri and F. Frascella, *Nanomaterials*, 2020, **10**, 1788.
- 159 G. Grigaleviciute, D. Baltriukiene, V. Bukelskiene and M. Malinauskas, *Coatings*, 2020, **10**, 254.
- 160 N.-K. Hwangbo, N.-E. Nam, J.-H. Choi and J.-E. Kim, *Polymer*, 2021, **13**, 4410.
- 161 C. Hart, C. M. Didier, F. Sommerhage and S. Rajaraman, *Biosensors*, 2020, **10**, 152.
- 162 K. Piironen, M. Haapala, V. Talman, P. Järvinen and T. Sikanen, *Lab Chip*, 2020, **20**, 2372–2382.
- 163 S. Krefß, R. Schaller-Ammann, J. Feiel, J. Friedl, C. Kasper and D. Egger, *Materials*, 2020, **13**, 3011.
- 164 D. Barata, E. Provaggi, C. van Blitterswijk and P. Habibovic, *Lab Chip*, 2017, **17**, 4134–4147.
- 165 L. T. Hirschwald, S. Brosch, G. Linz, J. Linkhorst and M. Wessling, *Adv. Mater. Technol.*, 2023, **8**, 2201857.

